arXiv:1608.05713v1 [hep-ph] 19 Aug 2016

ACFI-T16-22

A Tale of Two Twin Higgses: Addressing Little Hierarchy in Natural 2HDM Framework

Jiang-Hao Yu[†1]

[†] *Amherst Center for Fundamental Interactions, Department of Physics, University of Massachusetts Amherst, Amherst, MA 01002, USA*

Abstract

In original twin Higgs model, vacuum misalignment between electroweak and new physics scales is realized by adding explicit $\mathbb{Z}_2$ breaking term. Introducing additional twin Higgs could accommodate spontaneous $\mathbb{Z}_2$ breaking, which explains the origin of this misalignment. We introduce a class of two twin Higgs doublet models with most general scalar potential, and discuss general conditions which trigger electroweak and $\mathbb{Z}_2$ symmetry breaking. Various scenarios on realising the vacuum misalignment are systematically discussed in a natural two Higgs double model framework: explicit $\mathbb{Z}_2$ breaking, radiative $\mathbb{Z}_2$ breaking, tadpole-induced $\mathbb{Z}_2$ breaking, and quartic-induced $\mathbb{Z}_2$ breaking. We investigate the Higgs mass spectra and the Higgs phenomenology in these scenarios.

[1] jhyu@physics.umass.edu

1 Introduction

The discovery of a 125 GeV Higgs boson at the LHC [1, 2] is a great triumph of the Standard Model (SM) of particle physics. Although it confirms the Higgs mechanism, it sharpens existing naturalness problem. Naturalness tells us that the weak scale should be insensitive to quantum effects from physics at very higher scale. However, in SM, the large, quadratically divergent radiative corrections to the Higgs mass parameter destabilize the electroweak scale. From theoretical point of view, the SM should be well-behaved up to Planck scale. The existing hierarchy between the Planck and weak scales requires that the quantum corrections to the Higgs mass parameter should cancel against the Higgs bare mass to obtain the observed 125 GeV Higgs boson mass. The large cancellation indicates existence of fine-tuning between the tree-level Higgs mass parameter and loop-level Higgs mass corrections. This is the well-known hierarchy problem [3].

The dynamical solution to the naturalness problem is to introduce a new symmetry which protects the Higgs mass against large radiative corrections. Under this direction are weak scale supersymmetry [4], and composite Higgs [5–7], etc. These new physics (NP) models introduce symmetry partners of the SM fields that cancel the quadratically divergent corrections to the Higgs boson mass. Because the dominant quantum correction to the Higgs mass involves in the SM top quark in the self-energy loop, the top quark partner is typically most relevant new particle to the quadratic cancellation. The new symmetry not only relates the top partner with the SM top quark, but also relates the Higgs coupling of the top partner to the one of the top quark. This enforces quadratic cancellation between the top quark and top partner contributions. Since the top partners typically carry SM color charge, the search limits of these top partners at the LHC have reached 700$\sim$ 800 GeV. This already leads to around 10% level of tuning between the weak scale and NP scale. This is known as the little hierarchy problem.

One way to avoid the little hierarchy problem is the neutral naturalness [8–10], that symmetry partners are not charged under the SM gauge groups. This lowers the NP cutoff scale, and thus softens the little hierarchy problem. The twin Higgs model [8] [see also Refs. [11–15] and [21–23]] introduces the mirror copy of the SM, the twin sector, which is neutral under the SM gauge group. The Higgs sector respects the approximate global $U(4)$ symmetry, which is broken spontaneously to $U(3)$ at NP scale f. The $U(4)$ symmetry is broken at the loop level via radiative corrections from the gauge and Yukawa interactions. Thus the Higgs boson is the pseudo Goldstone Boson (PGB) of the symmetry breaking. Imposing a discrete $\mathbb{Z}_2$ symmetry between SM and twin sectors ensures that radiative corrections to the Higgs mass squared are still $U(4)$ symmetric. Thus there is no quadratically divergent radiative corrections to the Higgs mass terms. At the same time, the $\mathbb{Z}_2$ symmetry needs to be broken *at electroweak scale*. Otherwise, the $\mathbb{Z}_2$ symmetry induces symmetric VEVs at NP scale. It is necessary to realize have vacuum misalignment $v \ll f$ (and thus some level of little hierarchy) to separate the electroweak and NP scales. This implies a moderate amount of tuning (approximately $\frac{2v^2}{f^2}$).

If the Higgs boson is the PGB, the Higgs field should respect the shift symmetry. The shift symmetry is approximately broken by radiative corrections. Considering radiative corrections only, the typical Higgs potential [16] could be parametrized as

$$V(h) \simeq af^4 \sin^2 \frac{h}{f} + bf^4 \sin^4 \frac{h}{f}. \tag{1.1}$$

Here a and b denote radiative corrections, with the form

$$a \simeq b \simeq \frac{g_*^2}{(4\pi)^2} \log \frac{m_*^2}{f^2}, \tag{1.2}$$

where g_* denotes the typical SM couplings, such as top Yukawa coupling, and m_* represents the top partner mass. If there is no other contribution than the radiative corrections, the Higgs VEV can be obtained as

$$\langle h \rangle = \sqrt{a/b} f \simeq f. \tag{1.3}$$

To realize the vacuum misalignment, additional contributions need to be added to b or subtracted to a and have $a/b \simeq v^2/f^2$. In the littlest Higgs model [7], additional hard quartic terms are added to b by hand to enhance the b. Instead, one could introduce soft term to a to reduce a. In the original twin Higgs model, the $\mathbb{Z}_2$ symmetry is broken explicitly by introducing soft or hard $\mathbb{Z}_2$ breaking terms in the scalar potential. The soft mass term is added only to visible or twin sector to reduce a. To soften the tuning between v and f, the Higgs sector is extended to incorporate two twin Higgses. Refs. [17, 18] introduce two twin Higgses, and several choices of the soft mass terms are introduced to breaking the $\mathbb{Z}_2$ symmetry and reduces level of fine tuning. In the supersymmetric realization of the twin Higgs model [19, 20], two twin Higgses are also naturally introduced. In these literatures, the soft $\mathbb{Z}_2$ symmetry breaking term is introduced by hand, and its origin is unknown. Actually two twin Higgs setup provides more variants of $\mathbb{Z}_2$ symmetry breaking.

The spontaneous $\mathbb{Z}_2$ breaking mechanism provide a complete description of the electroweak symmetry breaking and vacuum misalignment. The two twin Higgses are necessary to obtain such spontaneous breaking mechanism, without introducing the explicit $\mathbb{Z}_2$ breaking term. Refs. [24, 25] discussed the tadpole induced spontaneous $\mathbb{Z}_2$ breaking by introducing the bilinear term between two twin Higgses. Without bilinear term, the VEVs of the first Higgs preserve $\mathbb{Z}_2$ while the other breaks it spontaneously. The bilinear Higgs mass term could transmit the $\mathbb{Z}_2$ breaking from the broken one to the unbroken one. It serves as the effective tadpole induced symmetry breaking and induces the vacuum misalignment naturally. Ref. [26] realized that the spontaneous $\mathbb{Z}_2$ breaking could be realized even without tree-level bilinear term, the "radiative $\mathbb{Z}_2$ breaking". In this scenario, both the symmetry breaking and $\mathbb{Z}_2$ breaking are obtained by opposite but comparable radiative corrections from the gauge and Yukawa arrangements. It seems that it is very hard to realize such radiative $\mathbb{Z}_2$ breaking, because typically the gauge corrections is much smaller than the Yukawa corrections, and thus the cancellation in the Higgs mass squared term is not adequate. But the gauge corrections could be enhanced by adjusting the VEVs of the two twin Higgses to be hierarchical. Through this way, the purely radiative corrections could induce spontaneous $\mathbb{Z}_2$ breaking.

In this work, we consider the general conditions which trigger the electroweak symmetry and the $\mathbb{Z}_2$ breaking. Both the tadpole-induced and radiative $\mathbb{Z}_2$ breaking scenarios could be deduced from the general conditions. We find that there is another novel spontaneous $\mathbb{Z}_2$ breaking mechanism. Instead of introducing the bilinear term in two twin Higgs potential, the quartic terms $\lambda_{4,5}$ could play the role of breaking $\mathbb{Z}_2$ symmetry spontaneously. This is the "quartic induced $\mathbb{Z}_2$ breaking". Similar to radiative symmetry breaking, the tree-level quartic terms $\lambda_{4,5}$ contribute to cancellation of the Higgs mass squared term. At the same time, similar to the tadpole-induced scenario, turning on $\lambda_{4,5}$ gradually transits the VEV of one Higgs to another one of another Higgs. Thus it provides another natural way to realize vacuum misalignment.

To systematically classify various $\mathbb{Z}_2$ breaking scenarios, we investigate the most general scalar potential in the two twin Higgs doublet framework. Integrating out the twin particles, the visible Higgs sector contains

the 2HDM scalar potential. Depending on the breaking pattern, the scalars in visible sector could be partially Goldstone Bosons or complete Goldstone bosons. Through the 2HDM framework, physics behind the spontaneous $\mathbb{Z}_2$ breaking scenarios could be explained. The above radiative, tadpole induced, and quartic induced symmetry breaking mechanisms are also classified and considered in a unified framework for the two twin Higgses. The collider phenomenology of the two twin Higgs models is quite similar to the one of 2HDM. Only when we see the signatures of the twin Higgses, we will be able to distinguish these two models.

The paper is organized as follows. In Section 2 we briefly review the original twin Higgs and the vacuum misalignment in this model. In Section 3 we introduce the most general scalar potential and its radiative corrections in the two twin Higgs model. Then we investigate the conditions for symmetry breaking and vacuum misalignment in Section 4. Subsequently in section 5 we classify various $\mathbb{Z}_2$ symmetry breaking scenarios in a natural two Higgs doublet framework. Section 6 discuss the Higgs phenomenology in each scenario. Finally we conclude this paper. In Appendix A and B, we list the calculation details of the two twin Higgs models.

2 Original Twin Higgs and Vacuum Misalignment

We first briefly review the twin Higgs model [8, 12–14] and how the vacuum misalignment is realized in this model. The original twin Higgs model consists of a mirror copy of the SM content, called the twin sector. We use the labels A and B to denote the SM and twin sector respectively. The twin sector is related to the SM sector by a $\mathbb{Z}_2$ exchange symmetry: $A \leftrightarrow B$. The Higgs sector consists of the SM Higgs doublet H_A and the twin Higgs doublet H_B. Due to the $\mathbb{Z}_2$ symmetry, the Higgs potential preserves an approximate global symmetry $U(4)$:

$$V_{\text{tree}} = -\mu^2(H_A^2 + H_B^2) + \lambda(H_A^2 + H_B^2)^2 = -\mu^2 H^2 + \lambda H^2, \tag{2.1}$$

with the $U(4)$ invariant field $H \equiv \begin{pmatrix} H_A \\ H_B \end{pmatrix}$. If the μ^2 is positive, the global $U(4)$ symmetry is spontaneously broken down to $U(3)$ and there are seven Goldstone Bosons modes. Assuming the VEV $\langle H \rangle = f$ lies along H_B, three Goldstone bosons are eaten by the twin gauge bosons, and the H_A remains massless. Assuming the radial model is heavy, the field H can be parametrized [1] nonlinearly as

$$H \equiv \begin{pmatrix} H_A \\ H_B \end{pmatrix} = \exp\left(\frac{i}{f}\Pi\right) \begin{pmatrix} 0 \\ 0 \\ 0 \\ \hline f \end{pmatrix}, \quad \Pi = \left(\begin{array}{ccc|c} 0 & 0 & 0 & h_1 \\ 0 & 0 & 0 & h_2 \\ 0 & 0 & 0 & h_3 \\ \hline h_1^* & h_2^* & h_3^* & h_0 \end{array}\right), \tag{2.3}$$

[1] Different notations on field definition and VEVs are used in literatures [8]. Here we define the field and take notation on field VEVs $\langle H_B \rangle = f$ and $\langle H_A \rangle = v = 174$ GeV. Using the same field definition, another notation on field VEVs $\langle H_B \rangle = f$ and $\langle H_A \rangle = v/\sqrt{2} = 174$ GeV are also used in literature [13]. Finally some literature [27] uses the following field definition

$$H \equiv \exp\left(\frac{i}{f}\Pi\right) \begin{pmatrix} 0 \\ 0 \\ 0 \\ \hline \frac{f}{\sqrt{2}} \end{pmatrix}, \quad \Pi = \left(\begin{array}{ccc|c} 0 & 0 & 0 & h_1 \\ 0 & 0 & 0 & h_2 \\ 0 & 0 & 0 & h_3 \\ \hline h_1^* & h_2^* & h_3^* & h_0 \end{array}\right), \tag{2.2}$$

Note that the normalization of the h_i is different, with $\text{Re}h_i + i\text{Im}h_i$ to have correct field normalization. Under this notation, the VEVs are $\langle H_B \rangle = f/\sqrt{2}$ and $\langle H_A \rangle = v/\sqrt{2} = 174$ GeV.

with $h_i = \frac{\mathrm{Re}h_i + i\mathrm{Im}h_i}{\sqrt{2}}$ to have correct field normalization. Expanding out the exponential and taking the unitary gauge we obtain the explicit form

$$H = \begin{pmatrix} f\frac{i\boldsymbol{h}}{\sqrt{\boldsymbol{h}^\dagger\boldsymbol{h}}}\sin\left(\frac{\sqrt{\boldsymbol{h}^\dagger\boldsymbol{h}}}{f}\right) \\ 0 \\ f\cos\left(\frac{\sqrt{\boldsymbol{h}^\dagger\boldsymbol{h}}}{f}\right) \end{pmatrix} \simeq \begin{pmatrix} i\boldsymbol{h} \\ 0 \\ f - \frac{1}{2f}\boldsymbol{h}^\dagger\boldsymbol{h} \end{pmatrix}, \tag{2.4}$$

where the field $\boldsymbol{h}$ denotes the SM Higgs doublet $\boldsymbol{h} = \begin{pmatrix} h^+ \\ h^0 \end{pmatrix}$.

The global symmetry $U(4)$ is explicitly broken once the SM and its mirror gauge group $\mathrm{SM}_A \times \mathrm{SM}_B$ are gauged, and the Yukawa interactions are introduced. Both the gauge and Yukawa interactions give rise to radiative corrections to the quadratic part of the scalar potential. The leading correction to the potential induced by gauging the $\mathrm{SM}_A \times \mathrm{SM}_B$ is

$$\Delta V \supset \frac{9\Lambda^2}{64\pi^2}\left(g_A^2 H_A^\dagger H_A + g_B^2 H_B^\dagger H_B\right) \xrightarrow{\mathbb{Z}_2 : g_A = g_B} \frac{9g^2\Lambda^2}{64\pi^2}\left(H_A^\dagger H_A + H_B^\dagger H_B\right), \tag{2.5}$$

where g_A and g_B are the gauge couplings of the $\mathrm{SM}_A \times \mathrm{SM}_B$ gauge group. Here if the $\mathbb{Z}_2$ symmetry is imposed, the leading corrections to the quadratic part of the scalar potential *accidentally* respect the original $U(4)$ symmetry. Thus corrections from the gauge sector cannot contribute to the masses of the Goldstone bosons. Similarly, consider the Yukawa sector by focusing on the top Yukawa couplings, which takes the form

$$-\mathcal{L} \supset y_A H_A q_A t_A + y_B H_B q_B t_B + h.c., \tag{2.6}$$

where $q_{A,B}$ and $t_{A,B}$ are the left-handed $SU(2)_{A,B}$ doublet quark and right-handed $SU(2)_{A,B}$ singlet top quark in the SM and twin sectors. The leading corrections take the form

$$\Delta V \supset \frac{-3\Lambda^2}{8\pi^2}\left(y_A^2 H_A^\dagger H_A + y_B^2 H_B^\dagger H_B\right) \xrightarrow{\mathbb{Z}_2 : y_A = y_B} \frac{-3y^2\Lambda^2}{8\pi^2}\left(H_A^\dagger H_A + H_B^\dagger H_B\right). \tag{2.7}$$

Similarly the $\mathbb{Z}_2$ symmetry ensures that the leading corrections respect the $U(4)$ symmetry. Therefore, there is no quadratically divergent contribution to the Higgs boson mass at one loop order.

Although the $\mathbb{Z}_2$ symmetry ensures the quadratically divergent corrections respect the $U(4)$ symmetry, the gauge and Yukawa interactions still breaks the $U(4)$ symmetry via the logarithmically divergent corrections. The leading logarithmically divergent corrections takes the form

$$\Delta V \supset \frac{3y^4}{16\pi^2}\left(|H_A|^4 \log\frac{\Lambda^2}{y^2|H_A|^2} + |H_B|^4 \log\frac{\Lambda^2}{y^2|H_B|^2}\right). \tag{2.8}$$

The sub-leading corrections proportional to g^4 takes the similar form with opposite sign. However, since both the squared mass and quartic coupling come from the same loop-suppressed corrections, the VEV is obtained to be at the scale f as mentioned in Introduction. This fact can be seen if we write the scalar potential including the radiative corrections, to good approximation, as

$$V_{\mathrm{tot}} = -\mu^2(|H_A|^2 + |H_B|^2) + \lambda(|H_A|^2 + |H_B|^2)^2 + \delta(|H_A|^4 + |H_B|^4), \tag{2.9}$$

Here δ denotes the small $U(4)$-violating but $\mathbb{Z}_2$-preserving loop corrections on the quartic potential, with $\delta \ll \lambda$. According to the Eq. 2.8, the Yukawa interactions lead to $\delta \simeq \frac{3y^4}{16\pi^2}\log\frac{\Lambda^2}{y^2 f^2}$, while the gauge interactions give $\delta \simeq -\frac{9g^4}{256\pi^2}\log\frac{\Lambda^2}{g^2 f^2}$. It is interesting to note that the symmetry breaking structure is controlled by the sign of the δ:

- if $\delta < 0$ (such as, only including loop corrections from the gauge interactions), the potential induces

$$\langle H_A \rangle = 0, \qquad \langle H_B \rangle = f, \tag{2.10}$$

  which breaks the $\mathbb{Z}_2$ symmetry spontaneously.

- if $\delta > 0$ (such as, adding loop corrections from the Yukawa interactions), the potential induces

$$\langle H_A \rangle = \frac{f}{\sqrt{2}}, \qquad \langle H_B \rangle = \frac{f}{\sqrt{2}}, \tag{2.11}$$

  which preserves the $\mathbb{Z}_2$ symmetry.

The original twin Higgs belongs to the second case: the vacuum is equally aligned with the two sectors.

In order to realize the symmetry breaking at the electroweak scale, the VEV must be misaligned to be asymmetry $\langle H_A \rangle = v \ll f$. This requires explicit $\mathbb{Z}_2$ symmetry breaking by adding

- either a soft $\mathbb{Z}_2$-breaking mass term

$$V_{\text{soft}} \supset m_A^2 |H_A|^2, \qquad \text{with } m_A^2 \sim \mathcal{O}\left(\frac{f^2}{16\pi^2}\right) \ll \mu^2, \tag{2.12}$$

- or a hard $\mathbb{Z}_2$-breaking quartic term

$$V_{\text{hard}} \supset \lambda_A |H_A|^4, \qquad \text{with } \lambda_A \sim \mathcal{O}(0.1) \ll \lambda. \tag{2.13}$$

The approximate $U(4)$ global symmetry is still valid since $\mu^2 \gg m_A^2$ and $\lambda \gg \lambda_A$. The $\mathbb{Z}_2$-breaking term pushes the VEVs: $\langle H_A \rangle \to v$ and $\langle H_B \rangle \to f$, which gives the vacuum misalignment. To obtain the correct VEV v, one needs to tune the $\mathbb{Z}_2$-breaking parameter.

In the case of the soft mass m_A^2, let us rewrite the scalar potential in terms of the Higgs doublet $\boldsymbol{h}$. Taking expansion on the Higgs doublets

$$|H_A|^2 \equiv f^2 \sin^2\left(\frac{\sqrt{\boldsymbol{h}^\dagger \boldsymbol{h}}}{f}\right) \simeq \boldsymbol{h}^\dagger \boldsymbol{h}, \qquad |H_B|^2 \equiv f^2 \cos^2\left(\frac{\sqrt{\boldsymbol{h}^\dagger \boldsymbol{h}}}{f}\right) \simeq f^2 - \boldsymbol{h}^\dagger \boldsymbol{h}. \tag{2.14}$$

we obtain the dominant Higgs potential

$$V(\boldsymbol{h}) \simeq \left(m_A^2 - \frac{3y^4 f^2}{8\pi^2} \log \frac{\Lambda^2}{y^2 f^2}\right) \boldsymbol{h}^\dagger \boldsymbol{h} + \frac{3y^4}{16\pi^2} \left(\log \frac{\Lambda^2}{y^2 f^2} + \log \frac{\Lambda^2}{y^2 \boldsymbol{h}^\dagger \boldsymbol{h}}\right) (\boldsymbol{h}^\dagger \boldsymbol{h})^2 + \mathcal{O}\left(\frac{(\boldsymbol{h}^\dagger \boldsymbol{h})^3}{f^2}\right). \tag{2.15}$$

If the m_A^2 is smaller than δf^2 term, the mass term could be negative, which induces electroweak symmetry breaking, and the Higgs boson h obtains its mass. We minimize the potential and obtain the electroweak VEV from the tadpole condition

$$\frac{v^2}{f^2} = 1 - \frac{m_A^2}{\delta f^2}, \tag{2.16}$$

with $\delta \simeq \frac{3y^4}{16\pi^2}$. To realize electroweak VEV, m_A^2 should be comparable to the δf^2 term. This implies a moderate tuning between δf^2 and m_A^2. We estimate the tuning using the following approximation:

$$\Delta_m = \left|\frac{2\delta m^2}{m_h^2}\right|^{-1} \simeq \frac{m_h^2}{2\delta f^2} \sim \frac{2v^2}{f^2}, \tag{2.17}$$

where $m_h = 125$ GeV. For a TeV scale f, this corresponds to around 15% tuning.

3 Two Twin Higgs Doublet Model

3.1 General Twin Higgs Potential

In this work, the visible sector is extended to the two Higgs doublet model, which is denoted as the 2HDM sector. The twin sector is exactly the mirror copy of the 2HDM sector and it is related to the 2HDM sector by the twin mirror parity $\mathbb{Z}_2$. It is convenient to label the 2HDM sector and its twin sector as A and B respectively. In the 2HDM, there are two Higgs doublets H_{1A} and H_{2A}. In the twin sector, two twin Higgs doublets H_{1B} and H_{2B} are introduced and they are mapped into the 2HDM Higgses via the twin parity: $H_{1B} \xrightarrow{\mathbb{Z}_2} H_{1A}$, $H_{2B} \xrightarrow{\mathbb{Z}_2} H_{2A}$. Similar to the original twin Higgs model, it is convenient to define the $U(4)$ invariant fields

$$H_1 \equiv \begin{pmatrix} H_{1A} \\ H_{1B} \end{pmatrix}, \qquad H_2 \equiv \begin{pmatrix} H_{2A} \\ H_{2B} \end{pmatrix}. \tag{3.1}$$

which respect the twin parity $\mathbb{Z}_2$.

The scalar pontential of the fields H_1 and H_2 is similar to the two Higgs doublet model. In the generalized two Higgs doublet framework, we write the general twin Higgs potential

$$\begin{aligned} V(H_1, H_2) \quad = \quad & -\mu_1^2|H_1|^2 - \mu_2^2|H_2|^2 + \lambda_1(|H_1|^2)^2 + \lambda_2(|H_2|^2)^2 + \lambda_3|H_1|^2|H_2|^2 \\ & + m_{12}^2\left[H_1^\dagger H_2 + h.c.\right] + \lambda_4|H_1^\dagger H_2|^2 + \frac{\lambda_5}{2}\left[(H_1^\dagger H_2)^2 + h.c.\right] \\ & + \left[(\lambda_6|H_1|^2 + \lambda_7|H_2|^2)H_1^\dagger H_2 + h.c.\right]. \end{aligned} \tag{3.2}$$

Here all the parameters are taken to be real for simplicity. Note that Refs. [17, 18] only contains $\lambda_{1,2,4}$ terms in the potential. The symmetries of the potential are recognised as follows:

- First, of course, all the terms in the potential preserves the twin parity $\mathbb{Z}_2$ symmetry: $A \leftrightarrow B$.
- The first line of the potential Eq. 3.2 has the global $U(4)_1 \times U(4)_2$ symmetry.
- While the second and the third lines of the Eq. 3.2 explicitly breaks the global symmetry $U(4)_1 \times U(4)_2 \to U(4)_V$. If λ_5 is zero but λ_4 is non-zero, an additional global $U(1)$ symmetry exists.

To avoid tree-level Higgs mediated flavor changing neutral current, similar to 2HDM, a softly-broken discrete symmetry $Z_2' : H_1 \to H_1$ $H_2 \to -H_2$ are imposed on the quartic terms, which implies that $\lambda_6 = \lambda_7 = 0$, whereas $m_{12}^2 \neq 0$ is still allowed.

The two Higgs sector is weakly gauged under the mirror SM gauge group. The gauge symmetry is applied [2] under

$$\begin{pmatrix} SU(2)_A \times U(1)_A & 0 \\ 0 & SU(2)_B \times U(1)_B \end{pmatrix} \subset U(4). \tag{3.3}$$

The covariant kinetic terms of the Higgs fields are written as

$$\mathcal{L}_{\text{kin}} = D_\mu H_1^\dagger D^\mu H_1 + D_\mu H_2^\dagger D^\mu H_2, \tag{3.4}$$

[2] To avoid massless twin photon, sometimes $U(1)_B$ gauge symmetry is not applied. Here we take the gauged $U(1)_B$.

where the covariant derivative is $D^\mu H_i = \partial^\mu H_i + igW^\mu H_i + ig'B^\mu H_i$, with

$$W^\mu \equiv \begin{pmatrix} W_A^{a\mu}\tau^a & 0 \\ 0 & W_B^{a\mu}\tau^a \end{pmatrix}, \quad B^\mu \equiv \begin{pmatrix} \frac{1}{2}B_A^\mu & 0 \\ 0 & \frac{1}{2}B_B^\mu \tau^a \end{pmatrix}. \tag{3.5}$$

The global symmetry is weakly broken by the loop effects from the gauge interactions.

If the mass terms $\mu_{1,2}^2$ are positive, the fields H_1 and H_2 vacua take the form

$$\langle H_1 \rangle \equiv \begin{pmatrix} 0 \\ 0 \\ 0 \\ f_1 \end{pmatrix}, \qquad \langle H_2 \rangle \equiv \begin{pmatrix} 0 \\ 0 \\ 0 \\ f_2 \end{pmatrix}. \tag{3.6}$$

Similar to the 2HDM model, let us define the mixing angle β and scale f

$$\tan\beta \equiv \frac{f_2}{f_1}, \quad f = \sqrt{f_1^2 + f_2^2}. \tag{3.7}$$

Depending on the global symmetry before the symmetry breaking, there could be seven or fourteen Goldstone bosons. In the following, we discuss the nonlinear parametrization of the fields H_i in $U(4)/U(3)$ and $[U(4)\times U(4)]/[U(3)\times U(3)]$ breaking patterns.

(1) $U(4)/U(3)$ Symmetry Breaking

The most general scalar potential in Eq. 3.2 exhibits the global $U(4)$ symmetry. The VEVs will break the symmetries of the Lagrangian spontaneously:

$$\begin{aligned} &\text{global symmetry:} && U(4) \to U(3), \\ &\text{gauge symmetry:} && SU(2)_A \times U(1)_A \times SU(2)_B \times U(1)_B \to SU(2)_A \times U(1)_A. \end{aligned} \tag{3.8}$$

The SUSY twin Higgs model [19, 20] belongs to this breaking pattern.

Similar to the original twin Higgs, there are seven Goldstone bosons. To isolate the Goldstone bosons in the fields, similar to 2HDM, it is convenient to work in the Higgs basis by rotating the fields

$$H = H_1\cos\beta + H_2\sin\beta, \qquad H' = -H_1\sin\beta + H_2\cos\beta, \tag{3.9}$$

After rotation, only the field H obtain VEV. Similar to the original twin Higgs, the field H can be parametrized non-linearly. After rotation, the two fields becomes

$$H = \exp\left[\frac{i}{f}\left(\begin{array}{c|cc} \mathbf{0}_{2\times 2} & \mathbf{0}_{1\times 2} & \boldsymbol{h} \\ \hline \mathbf{0}_{2\times 1} & 0 & C \\ \boldsymbol{h}^* & C^* & N \end{array}\right)\right]\left(\begin{array}{c} \mathbf{0}_{1\times 2} \\ \hline 0 \\ f \end{array}\right), \quad H' = \begin{pmatrix} H^+ \\ H^0 + iA^0 \\ H'^+ \\ H'^0 + iA'^0 \end{pmatrix}. \tag{3.10}$$

where the field $\boldsymbol{h}$ denotes the SM Higgs doublet $\boldsymbol{h} = \begin{pmatrix} h^+ \\ h^0 \end{pmatrix}$, and $C^\pm$ and N are Goldstone bosons in the B sector, which is absorbed by the twin gauge bosons. Therefore, similar to the original twin Higgs, taking the expansion, the field H takes the form

$$H = \begin{pmatrix} f\frac{i\boldsymbol{h}}{\sqrt{\boldsymbol{h}^\dagger\boldsymbol{h}}}\sin\left(\frac{\sqrt{\boldsymbol{h}^\dagger\boldsymbol{h}}}{f}\right) \\ 0 \\ f\cos\left(\frac{\sqrt{\boldsymbol{h}^\dagger\boldsymbol{h}}}{f}\right) \end{pmatrix} \simeq \begin{pmatrix} i\boldsymbol{h} \\ 0 \\ f - \frac{1}{2f}\boldsymbol{h}^\dagger\boldsymbol{h} \end{pmatrix}, \tag{3.11}$$

Here the field H plays the role of the twin Higgs as the original twin Higgs model. Another field H' does not obtain VEV, and thus it is just another scalar quadruplet in this model.

(2) $[U(4)\times U(4)]/[U(3)\times U(3)]$ Symmetry Breaking

Now let us consider the special scalar potential with larger global symmetry. If only the first line exists, The potential exhibits the exact global $U(4)\times U(4)$ symmetry. Here the soft mass term m_{12}^2 and the quartic λ_4 and λ_5 terms are taken to be small, and thus the $U(4)\times U(4)$ symmetry becomes approximate. The VEVs will break the symmetries of the Lagrangian spontaneously:

$$\begin{aligned} &\text{global symmetry:} && U(4)\times U(4)\to U(3)\times U(3),\\ &\text{gauge symmetry:} && SU(2)_A\times U(1)_A\times SU(2)_B\times U(1)_B\to SU(2)_A\times U(1)_A. \end{aligned} \tag{3.12}$$

In this case, the approximate global symmetry breaking is $U(4)_1\times U(4)_2\to U(3)_1\times U(3)_2$. Let us parametrize the fields H_1 and H_2 nonlinearly in terms of the nonlinear sigma field. Assuming the radial models ρ_1 and ρ_2 in H_1 and H_2 are heavy, the fields H_1 and H_2 are parametrized nonlinearly as

$$H_1=\exp\left[\frac{i}{f_1}\left(\begin{array}{c|cc} \mathbf{0}_{2\times2} & \mathbf{0}_{1\times2} & \boldsymbol{h}_1\\ \hline \mathbf{0}_{2\times1} & 0 & C_1\\ \boldsymbol{h}_1^* & C_1^* & N_1 \end{array}\right)\right]\left(\begin{array}{c} \mathbf{0}_{1\times2}\\ \hline 0\\ f_1 \end{array}\right),\quad H_2=\exp\left[\frac{i}{f_2}\left(\begin{array}{c|cc} \mathbf{0}_{2\times2} & \mathbf{0}_{1\times2} & \boldsymbol{h}_2\\ \hline \mathbf{0}_{2\times1} & 0 & C_2\\ \boldsymbol{h}_2^* & C_2^* & N_2 \end{array}\right)\right]\left(\begin{array}{c} \mathbf{0}_{1\times2}\\ \hline 0\\ f_2 \end{array}\right) \tag{3.13}$$

Expanding out the exponential we obtain the explicit form

$$H_i=\begin{pmatrix} f_i\frac{i\boldsymbol{h}_i}{\mathbb{H}_i}\sin\left(\frac{\mathbb{H}_i}{f_i}\right)\\ f_i\frac{iC_i}{\mathbb{H}_i}\sin\left(\frac{\mathbb{H}_i}{f_i}\right)\\ f_i\cos\left(\frac{\mathbb{H}_i}{f_i}\right)+f\frac{iN_i}{\mathbb{H}_i}\sin\left(\frac{\mathbb{H}_i}{f_i}\right) \end{pmatrix}\simeq\begin{pmatrix} i\boldsymbol{h}_i\\ iC_i\\ f_i-\frac{1}{2f}\boldsymbol{h}_i^\dagger\boldsymbol{h}_i+iN_i \end{pmatrix}, \tag{3.14}$$

where $\mathbb{H}_i=\sqrt{\boldsymbol{h}_i^\dagger\boldsymbol{h}_i+C_i^*C_i+N_i^2}$. Here the doublets $\boldsymbol{h}_i=\begin{pmatrix} h_i^+\\ h_i^0\end{pmatrix}$ are Goldstone bosons in the sector A, and C_i, N_i are Goldstone bosons in the sector B. When $U(4)\times U(4)$-breaking terms exist, one combination of the $h_i^\pm$, and one combination of the $C_i^\pm$ becomes pseudo Goldstone bosons.

3.2 Fermion Assignments

In the twin Higgs model, the SM fermions are extended to include mirror fermions:

$$\begin{aligned} q_A(3,2,1/6;1,1,0) &\xrightarrow{\mathbb{Z}_2} q_B(1,1,0;3,2,1/6),\\ u_A(3,1,2/3;1,1,0) &\xrightarrow{\mathbb{Z}_2} u_B(1,1,0;3,1,2/3),\\ d_A(3,1,-1/3;1,1,0) &\xrightarrow{\mathbb{Z}_2} d_B(1,1,0;3,1,-1/3), \end{aligned} \tag{3.15}$$

where the quantum number assignments are $(SU(3)_A, SU(2)_A, U(1)_A; SU(3)_B, SU(2)_B, U(1)_B)$. If there are two twin Higgses, the general Yukawa interactions could be written as

$$-\mathcal{L}_{\text{Yuk}}=y_1\left(q_AH_{1A}t_A+q_BH_{1B}t_B\right)+(1\leftrightarrow2)+h.c. \tag{3.16}$$

Similar to 2HDM, it is possible to induce Higgs mediated FCNC processes in visible sector. To avoid such problem, the discrete Z_2' symmetry $H_1\to H_1, H_2\to -H_2$ can also be applied to the fermion contents, which are identified as the Type-I, II, X, Y 2HDMs [28]. Here for simplicity, we adopt the type-I Yukawa structure:

all fermions only couple with H_1. Similar to 2HDM, it is straightforward to extend type-I Yukawa structure to other Yukawa structures.

(1) Fermion Assignment: Mirror Fermions

In this setup, similar to the original twin Higgs model, the 2HDM top Yukawa interactions are

$$-\mathcal{L}_{\rm Yuk} = y\left(q_A H_{1A} t_A + q_B H_{1B} t_B\right) + h.c. \tag{3.17}$$

In the above Lagrangian the $U(4)$ symmetry is explicitly broken by the Yukawa terms. Similar to the SM fermions, the mirror fermions are treated as the chiral fermions. The fermion masses are

$$m_{t_A}^2 = y^2 H_{1A}^2, \qquad m_{t_B}^2 = y^2 H_{1B}^2 \simeq y^2 f^2 - y^2 H_{1A}^2, \tag{3.18}$$

where the relation $m_{t_A}^2 + m_{t_B}^2 \simeq y^2 f^2$ indicates the quadratically divergent cancellation. Of course, it is also possible to treat the mirror fermions vector-like [29] with

$$-\mathcal{L}_{\rm mass} = M(q_B q_B + t_B t_B) + h.c. \tag{3.19}$$

Here additional fermion degree of freedoms are introduced to make the mirror fermions vector-like. This will lift the mirror fermion masses but not affect the quadratically divergent cancellation in the Higgs potential. Here we only take chiral fermion case.

(2) Fermion Assignment: $SU(6) \times SU(4)$ Fermions

To keep the $U(4)$ invariant form, the following fermions [8] are introduced:

$$\begin{aligned}
Q &= q_A\left(3,2,1/6;1,1,0\right) + \tilde{q}_A\left(3,1,2/3;1,2,-1/2\right) + q_B\left(1,1,0;3,2,1/6\right) + \tilde{q}_B(1,2,-1/2;3,1,2/3), \\
U &= t_A\left(3,1,2/3;1,1,0\right) + t_B\left(1,1,0;3,1,2/3\right), \\
D &= b_A\left(3,1,-1/3;1,1,0\right) + b_B\left(1,1,0;3,1,-1/3\right).
\end{aligned} \tag{3.20}$$

In the $SU(6) \times SU(4)$ invariant form, the fermions are assembled as

$$Q = \begin{pmatrix} q_A & \tilde{q}_A \\ \tilde{q}_B & q_B \end{pmatrix}, \qquad U = \begin{pmatrix} t_A \\ t_B \end{pmatrix}. \tag{3.21}$$

Similar for the leptons. The $U(4) \times U(4)$ invariant top Yukawa interactions are written as

$$-\mathcal{L}_{\rm Yuk} = y H_1^\dagger Q U + h.c. = \begin{pmatrix} H_{1A} & H_{1B} \end{pmatrix} \begin{pmatrix} q_A & \tilde{q}_A \\ \tilde{q}_B & q_B \end{pmatrix} \begin{pmatrix} t_A \\ t^B \end{pmatrix} + h.c. \tag{3.22}$$

To lift the non-SM fermions masses, additional vector-like fermion mass terms are introduced as

$$-\mathcal{L}_{\rm mass} = M(q_B q_B + t_B t_B) + \tilde{M}(\tilde{q}_A \tilde{q}_A + \tilde{q}_B \tilde{q}_B) + h.c. \tag{3.23}$$

The vector-like mass terms exhibit $U(4) \times U(4)$ breaking effects in the Yukawa sector.

Expanding the Yukawa interactions, we obtain

$$-\mathcal{L}_{\rm Yuk} = y\left(q_A H_{1A} t_A + q_B H_{1B} t_B + H_{1A} \tilde{q}_B t_B + H_{1B} \tilde{q}_A t_A\right) + h.c. \tag{3.24}$$

Thus the mass matrices are

$$-\mathcal{L}_{\rm mass} = \begin{pmatrix} q_A & \tilde{q}_A \end{pmatrix} \begin{pmatrix} H_{1A} & 0 \\ H_{1B} & \tilde{M} \end{pmatrix} \begin{pmatrix} t_A \\ \tilde{q}_A \end{pmatrix} + \begin{pmatrix} q_B & \tilde{q}_B \end{pmatrix} \begin{pmatrix} H_{1B} & 0 \\ H_{1A} & \tilde{M} \end{pmatrix} \begin{pmatrix} t_B \\ \tilde{q}_B \end{pmatrix} + h.c. \tag{3.25}$$

3.3 Radiative Corrections

The gauge and Yukawa interactions break the global symmetry explicitly, which generates the scalar potential for the pseudo-Goldstonbe bosons. The one-loop Coleman-Weinberg potential in Landau gauge is

$$V_{\rm CW}(H_1,H_2)=\frac{1}{64\pi^2}{\rm STr}\left[m^4(H_{1,2})\log\frac{m^2(H_{1,2})}{\Lambda^2}-\frac{3}{2}\right], \tag{3.26}$$

where the super-trace STr is taken among all the dynamical fields that have the Higgs dependent masses. The Higgs dependent gauge boson masses are

$$m^2_{W_A}=\frac{g^2}{2}\left(|H_{1A}|^2+|H_{2A}|^2\right),\qquad m^2_{W_B}=\frac{g^2}{2}\left(|H_{1B}|^2+|H_{2B}|^2\right), \tag{3.27}$$

for the $SU(2)\times SU(2)$ gauge bosons, and similarly for the $U(1)\times U(1)$ gauge boson masses. The Higgs dependent top sector masses in the fermion assignment I are

$$m^2_{t_A}=y^2|H_{1A}|^2,\qquad m^2_{t_B}=y^2|H_{1B}|^2. \tag{3.28}$$

The field dependent top sector masses in the fermion assignment II are

$$\begin{aligned} m^2_{t_A,t'_A} &= \frac{y^2|H_{1A}|^2+y^2|H_{1B}|^2+M^2}{2}\mp\frac{1}{2}\sqrt{(y^2|H_{1A}|^2+y^2|H_{1B}|^2+M^2)^2-4y^2|H_{1A}|^2M^2},\\ m^2_{t_B,t'_B} &= \frac{y^2|H_{1A}|^2+y^2|H_{1B}|^2+M^2}{2}\mp\frac{1}{2}\sqrt{(y^2|H_{1A}|^2+y^2|H_{1B}|^2+M^2)^2-4y^2|H_{1B}|^2M^2}. \end{aligned} \tag{3.29}$$

Let us examine that how the quadratic divergence cancels at the one-loop again due to the $\mathbb{Z}_2$ symmetry. The leading corrections to the quadratic part of the scalar potential are

$$\Delta V\supset\frac{9g^2\Lambda^2}{64\pi^2}\left(H^\dagger_{1A}H_{1A}+H^\dagger_{1B}H_{1B}+H^\dagger_{2A}H_{2A}+H^\dagger_{2B}H_{2B}\right), \tag{3.30}$$

from the gauge sector, and

$$\Delta V\supset\frac{-3y^2\Lambda^2}{8\pi^2}\left(H^\dagger_{1A}H_{1A}+H^\dagger_{1B}H_{1B}\right), \tag{3.31}$$

due to the Yukawa interactions in the top sector. Note that both quadratic contributions respect the original $U(4)$ symmetry, and thus there is no quadratically divergent contribution to the Higgs boson masses. Therefore the leading corrections are the quartic terms in the effective potential. The radiative corrections to the gauge sector is

$$\Delta V\supset\frac{3g^4}{16\pi^2}\left[\left(|H_{1A}|^2+|H_{2A}|^2\right)^2\log\frac{\Lambda^2}{g^2(|H_{1A}|^2+|H_{2A}|^2)}+\left(|H_{1B}|^2+|H_{2B}|^2\right)^2\log\frac{\Lambda^2}{g^2(|H_{1B}|^2+|H_{2B}|^2)}\right] \tag{3.32}$$

Similar for the $U(1)$ sector. The radiative corrections to the top sector in the mirror fermion model

$$\Delta V\supset\frac{3y^4}{16\pi^2}\left[\left(|H_{1A}|^2\right)^2\log\frac{\Lambda^2}{g^2|H_{1A}|^2}+\left(|H_{1B}|^2\right)^2\log\frac{\Lambda^2}{g^2|H_{1B}|^2}\right]. \tag{3.33}$$

In most general case, the dominant contributions of the radiative corrections could be parametrized as

$$\begin{aligned} V_{\rm rad.cor.} &= \delta_1\left(|H_{1A}|^4+|H_{1B}|^4\right)+\delta_2\left(|H_{2A}|^4+|H_{2B}|^4\right)+\delta_3\left(|H_{1A}|^2|H_{2A}|^2+|H_{1B}|^2|H_{2B}|^2\right)\\ &+ \delta_4\left(|H^\dagger_{1A}H_{2A}|^2+|H^\dagger_{1B}H_{2B}|^2\right)+\frac{\delta_5}{2}\left[(H^\dagger_{1A}H_{2A})^2+(H^\dagger_{1B}H_{2B})^2+h.c.\right]. \end{aligned} \tag{3.34}$$

Note that there could have $\delta_{6,7}$ terms in the scalar potential (just like the $\lambda_{6,7}$ terms in 2HDM). However, since we have taken the $\lambda_{6,7}$ terms to be zero, and we adopt the Type-I Yukawa structure, the radiative corrections could not generate $\delta_{6,7}$ terms. According to the effective potential, we list the the coefficients in Eq. 3.34:

$$\begin{aligned}
\delta_1 &\simeq -\frac{1}{16\pi^2}\left(\frac{9}{4}g^4+\frac{3}{2}g^2g'^2+\frac{3}{4}g'^4\right)\log\frac{\Lambda^2}{f^2},\\
\delta_2 &\simeq -\frac{1}{16\pi^2}\left(\frac{9}{4}g^4+\frac{3}{2}g^2g'^2+\frac{3}{4}g'^4\right)\log\frac{\Lambda^2}{f^2},\\
\delta_3 &\simeq -\frac{1}{16\pi^2}\left(\frac{9}{2}g^4-3g^2g'^2+\frac{3}{2}g'^4\right)\log\frac{\Lambda^2}{f^2},\\
\delta_4 &\simeq -\frac{1}{16\pi^2}\left(6g^2g'^2\right)\log\frac{\Lambda^2}{f^2},\\
\delta_5 &= 0.
\end{aligned} \tag{3.35}$$

from gauge interactions [17]. In the Type-I Yukawa structure, the Yukawa interactions induce

$$\delta_1 \simeq +\frac{1}{16\pi^2}(3y^4)\log\frac{\Lambda^2}{f^2}, \quad \delta_{2,3,4,5}=0, \tag{3.36}$$

for the fermion assignment I and

$$\delta_1 \simeq -\frac{3}{16\pi^2}\frac{y^2M^2/f^2}{M^2-y^2f^2}\left(M^2\log\frac{M^2+y^2f^2}{M^2}-y^2f^2\log\frac{M^2+y^2f^2}{y^2f^2}\right), \quad \delta_{2,3,4,5}=0, \tag{3.37}$$

for the fermion assignment II [8]. In other Yukawa structures, the Yukawa radiative corrections could be different. Here we neglect other non-logarithm contributions and small radiative contributions from scalar self-interactions.

The overall radiative corrections are the sum over gauge boson and fermion contributions. Note that the above radiative corrections are independent of the breaking patterns. It is valid for both both $U(4)/U(3)$ and $[U(4)\times U(4)]\,/\,[U(3)\times U(3)]$ pattern. Given the gauge and fermion assignments, the radiative corrections is completely determined by gauge and Yukawa couplings. In the following, we take general form of δ_{1-5}. In the numerical calculation, we take the values from the fermion assignments I:

$$\delta_1=0.09, \quad \delta_2=-0.004, \quad \delta_3=-0.005 \quad \delta_4=-0.002 \quad \delta_5=0, \quad \text{(benchmark point)}. \tag{3.38}$$

This serves as our benchmark point in the following discussions.

4 Symmetry Breaking and Vacuum Misalignment

The radiative corrections further trigger spontaneous symmetry breaking, and induce VEVs for the h_1^0 and h_2^0 components in $H_{1A,2A}$ defined in Eq. 3.13. We could determine the VEVs of $h_{1,2}^0$ in terms of general tadpole conditions from most general scalar potential. We find that the symmetry breaking and vacuum misalignment is quite sensitive to the global symmetry breaking patterns. Thus we will discuss the symmetry breaking and vacuum misalignment in both $U(4)/U(3)$ and $[U(4)\times U(4)]\,/\,[U(3)\times U(3)]$ breaking patterns.

4.1 $U(4)/U(3)$ Breaking Pattern

In this breaking pattern, due to the existence of the m_{12}^2 term and λ_{4-5} terms in the potential, the global symmetry breaking pattern is $U(4) \to U(3)$, with seven Goldstone bosons generated. The δ_{1-5} terms further trigger spontaneous symmetry breaking, and cause the Goldstone bosons become PGBs.

The radiative corrections from the gauge and Yukawa interactions trigger electroweak symmetry breaking. According to Eq. 3.10, only one combination of the twin Higgses $H_{1,2}$ obtain the VEV. Denoting the VEV $\theta \equiv \frac{\langle h^0 \rangle}{f}$ we have the field VEVs in the Higgs basis, or the $H_{1,2}$ basis:

$$\langle H \rangle = \begin{pmatrix} 0 \\ f \sin\theta \\ 0 \\ f \cos\theta \end{pmatrix}, \quad \langle H' \rangle \equiv 0, \qquad \text{or} \qquad \langle H_1 \rangle \equiv \begin{pmatrix} 0 \\ f_1 \sin\theta \\ 0 \\ f_1 \cos\theta \end{pmatrix}, \quad \langle H_2 \rangle \equiv \begin{pmatrix} 0 \\ f_2 \sin\theta \\ 0 \\ f_2 \cos\theta \end{pmatrix}. \tag{4.1}$$

Let us calculate the VEV $\theta = \langle h^0 \rangle / f$ using the tadpole conditions. The full tadpole conditions are listed in the Appendix A. The tadpole conditions not only determine the mass-squared parameters $\mu_{1,2}^2$, but also tell us the value of the VEV θ. Here we only list the tadpole conditions which determines the VEV:

$$\begin{aligned} \left(f_1^2 \delta_1 + f_2^2 \delta_{345}\right) \cos 2\theta &= 0, \\ \left(f_2^2 \delta_2 + f_1^2 \delta_{345}\right) \cos 2\theta &= 0. \end{aligned} \tag{4.2}$$

If $f_1 \neq f_2$ and $\delta_1 \neq \delta_2$, the two conditions lead to

$$\cos(2\theta) = 0 \qquad \Rightarrow \qquad \theta = \frac{\pi}{4} \qquad \Rightarrow \qquad \langle H_A \rangle = \langle H_B \rangle = f/\sqrt{2}. \tag{4.3}$$

The VEVs are equally aligned because of the $\mathbb{Z}_2$ symmetry. Similar to the original twin Higgs model, adding the soft or hard breaking terms could realize vacuum misalignment. Here we add the soft mass breaking terms in the scalar potential

$$V_{\text{soft}} = -m_{1A}^2 |H_{1A}|^2 - m_{2A}^2 |H_{2A}|^2 - m_{12A}^2 \left[H_{1A}^\dagger H_{2A} + h.c. \right]. \tag{4.4}$$

Taking the soft breaking terms into account, the relevant tadpole conditions become

$$\begin{aligned} F_{1A} + \left(2\delta_1 + t_\beta^2 \delta_{345}\right) \cos 2\theta &= 0, \\ F_{2A} + \left(2t_\beta^2 \delta_2 + \delta_{345}\right) \cos 2\theta &= 0. \end{aligned} \tag{4.5}$$

where $F_{1A} = \frac{m_{1A}^2 + m_{12A}^2 t_\beta^2}{f_1^2}$ and $F_{2A} = \frac{m_{2A}^2 + t_\beta^{-1} m_{12A}^2}{f_1^2}$. From the above relations we see that θ could be less than $\pi/4$ only if there are relations

$$F_{1A} \left(2t_\beta^2 \delta_2 + \delta_{345}\right) = F_{2A} \left(2\delta_1 + t_\beta^2 \delta_{345}\right), \qquad -F_{1A} < \left(2\delta_1 + t_\beta^2 \delta_{345}\right). \tag{4.6}$$

These could be easily satisfied, because both F_{1A} and F_{2A} are free parameters. Fig. 1 (left) shows the relations between between F_{1A} and F_{2A} given the t_β and benchmark parameters in Eq. 3.38. Given the soft mass term F_{1A} or F_{2A}, we could determine the VEV θ using tadpole conditions in Eq. 4.5. Fig. 1 (middle) shows that given the F_{1A} or F_{2A}, values of the θ for different $\tan\beta$. The Figure shows the solution $\theta < \pi/4$ exist, and thus the vacuum misalignment is realized.

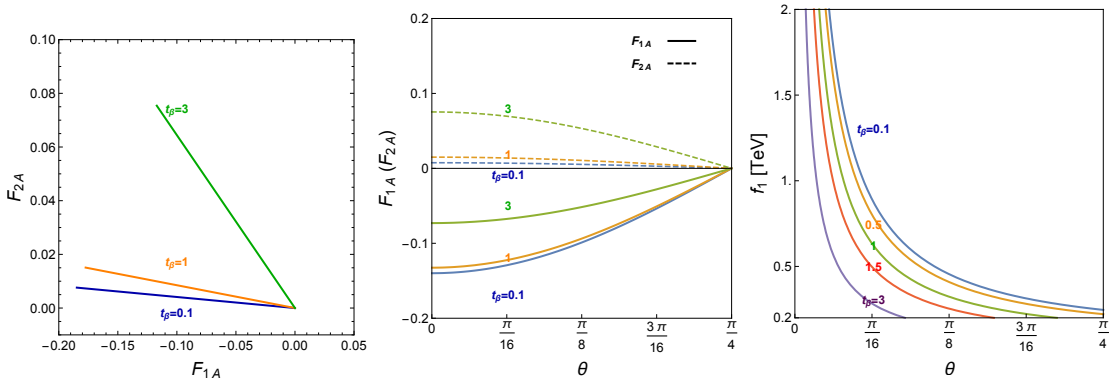

Figure 1: The left sub-figure shows the correlation between F_{1A} and F_{2A} for different t_β On the middle, it shows the F_{1A} (solid lines) and F_{2A} (dashed lines) as function of θ for different t_β. On the right, it shows the scale f_1 as function of θ for different t_β. Here the benchmark parameters δ_{1-5} in Eq. 3.38 are used.

Although the tadpole conditions in Eq. 4.5 determines θ, but to obtain VEV v, we need to know the scale f. To obtain the VEV at electroweak scale, the following condition should be imposed

$$f \sin\theta = f_1 \sqrt{1+t_\beta^2} \sin\theta = v = 174\,\text{GeV}. \tag{4.7}$$

Given fixed $\tan\beta$, there are relations between θ and f_1. The relation is shown in Fig. 1 (right), which plots the (θ, f_1) contours for various t_β. In summary, given appropriate values of m_{1A}^2 (or m_{2A}^2) and t_β, θ and f_1 are totally determined, and the vacuum misalignment with electroweak vacuum is realized.

4.2 $[U(4)\times U(4)]\,/\,[U(3)\times U(3)]$ Breaking Pattern

If the tree-level breaking terms are small, the potential exhibits approximate $U(4)\times U(4)$ global symmetry and exact $\mathbb{Z}_2$ symmetry. In the global symmetry breaking pattern $[U(4)\times U(4)]\,/\,[U(3)\times U(3)]$, 14 Goldstone bosons are generated after symmetry breaking. The δ_{1-5} terms further trigger spontaneous symmetry breaking, and cause the Goldstone bosons become PGBs.

The gauge and Yukawa interactions radiatively generate the symmetry breaking for the Goldstone bosons $\langle h_{1,2}\rangle$. Denoting

$$\theta_1 \equiv \frac{\langle h_1\rangle}{f_1}, \quad \theta_2 \equiv \frac{\langle h_2\rangle}{f_2}, \tag{4.8}$$

we parametrize the VEVs of the fields $H_{1,2}$ as

$$\langle H_1\rangle \equiv \begin{pmatrix} 0 \\ f_1\sin\theta_1 \\ 0 \\ f_1\cos\theta_1 \end{pmatrix}, \qquad \langle H_2\rangle \equiv \begin{pmatrix} 0 \\ f_2\sin\theta_2 \\ 0 \\ f_2\cos\theta_2 \end{pmatrix}. \tag{4.9}$$

The tadpole conditions not only determines the mass-squared parameters $\mu_{1,2}^2$, but also VEVs $\theta_{1,2}$. The full tadpole conditions are presented in Appendix B. Here we only list the two tadpole conditions which

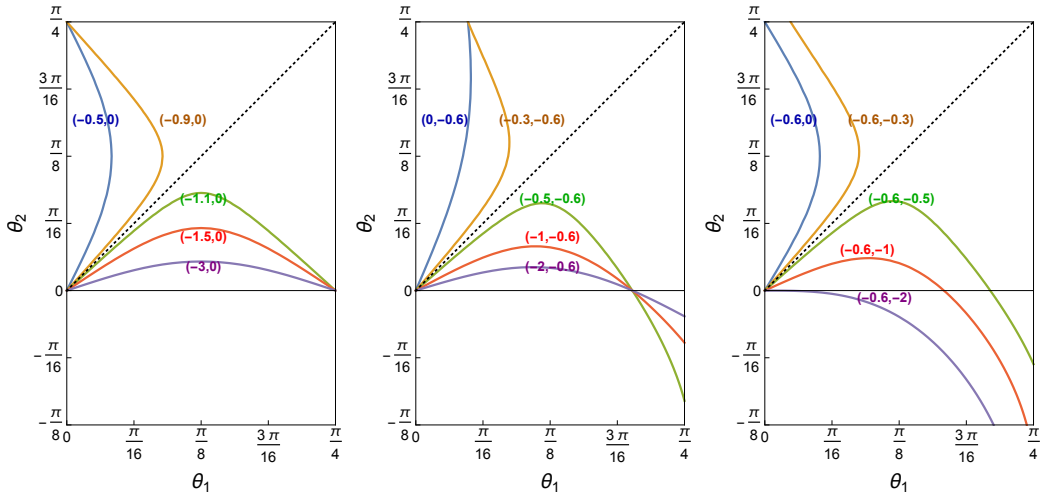

Figure 2: The contour lines show the relation between (θ_1, θ_2) imposed by the first tadpole condition in Eq. 4.10. Each contour is labeled by the radiative parameters (Ω_1, Ω_2). The left (middle) panel shows contours for different Ω_1 with $\Omega_2 = 0(-0.6)$. The right panel shows contours for different Ω_2 with $\Omega_1 = -0.6$.

determine the VEVs:

$$\begin{aligned}
&\sin 4\theta_1 + \Omega_1 \sin 4\theta_2 + \Omega_2 \sin 2(\theta_1 + \theta_2) = 0, \\
&\sin 4\theta_1 - \Omega_1 \sin 4\theta_2 + \Omega_2 \sin 2(\theta_1 - \theta_2) + 2F_\lambda \sin 2(\theta_1 - \theta_2) - 4F_m \sin(\theta_1 - \theta_2) = 0,
\end{aligned} \tag{4.10}$$

where we denote

$$\Omega_1 \equiv t_\beta^4 \frac{\delta_2}{\delta_1}, \quad \Omega_2 \equiv t_\beta^2 \frac{\delta_{345}}{\delta_1}, \quad F_\lambda \equiv t_\beta^2 \frac{\lambda_{45}}{\delta_1}, \quad F_m \equiv t_\beta \frac{m_{12}^2}{\delta_1 f_1^2}. \tag{4.11}$$

In Ref. [24], only Ω_1 and m_{12}^2 terms are included in the tadpole conditions. Thus the tadpole conditions in Ref. [24] could be treated as a special case of this general discussion. Note that parameters (Ω_1, Ω_2) only depend on t_β and radiative corrections, denoted as "radiative breaking parameters". (Ω_1, Ω_2) are uniquely determined once we know the gauge and fermion assignments. In Type-I fermion assignment, we have $\delta_1 > 0$ and $\delta_{2-5} < 0$. This indicates $\Omega_1 < 0$ and $\Omega_2 < 0$. In the following, we will focus on the region $\Omega_1 < 0$ and $\Omega_2 < 0$ [3]. On the other hand, (F_λ, F_m) depend on both radiative parameters and tree-level $U(4) \times U(4)$ breaking terms λ_{45} and m_{12}^2, denoted as "tree breaking parameters". Given radiative and tree-level breaking parameters, (θ_1, θ_2) are uniquely determined by the tadpole conditions.

The first tadpole condition in Eq. 4.10 tells us the relation between θ_1 and θ_2. In Fig. 2 we plot the correlation between (θ_1, θ_2) for different (Ω_1, Ω_2) . Several features are in order. First, depending on the size of $|\Omega_1 + \Omega_2|$, the contours live in regions: $\theta_2 < \theta_1$ for $|\Omega_1 + \Omega_2| > 1$, and $\theta_2 > \theta_1$ for $|\Omega_1 + \Omega_2| < 1$. Second, Ω_2 determines intersection point θ_1^* between the contour curve and the x-axis, or θ_2^* between the curve and y-axis. If Ω_2 is zero, the intersection point is either $\theta_1^* = \pi/4$ or $\theta_2^* = \pi/4$. From Fig. 2 (right), the smaller Ω_2, the smaller θ_1^* if $|\Omega_1 + \Omega_2| > 1$, while the larger θ_2^* if $|\Omega_1 + \Omega_2| < 1$. Third, Ω_1 only controls the

[3] If $\Omega_1 < 0, \Omega_2 > 0$ or $\Omega_1 > 0, \Omega_2 < 0$, the $\mathbb{Z}_2$ symmetry breaking could also be realized. For example, if $\Omega_1 < 0, \Omega_2 > 0$, the $\mathbb{Z}_2$ symmetry breaking happens when $\theta_1 < \theta_2 < \pi/4$. This could happen in a different fermion assignments.

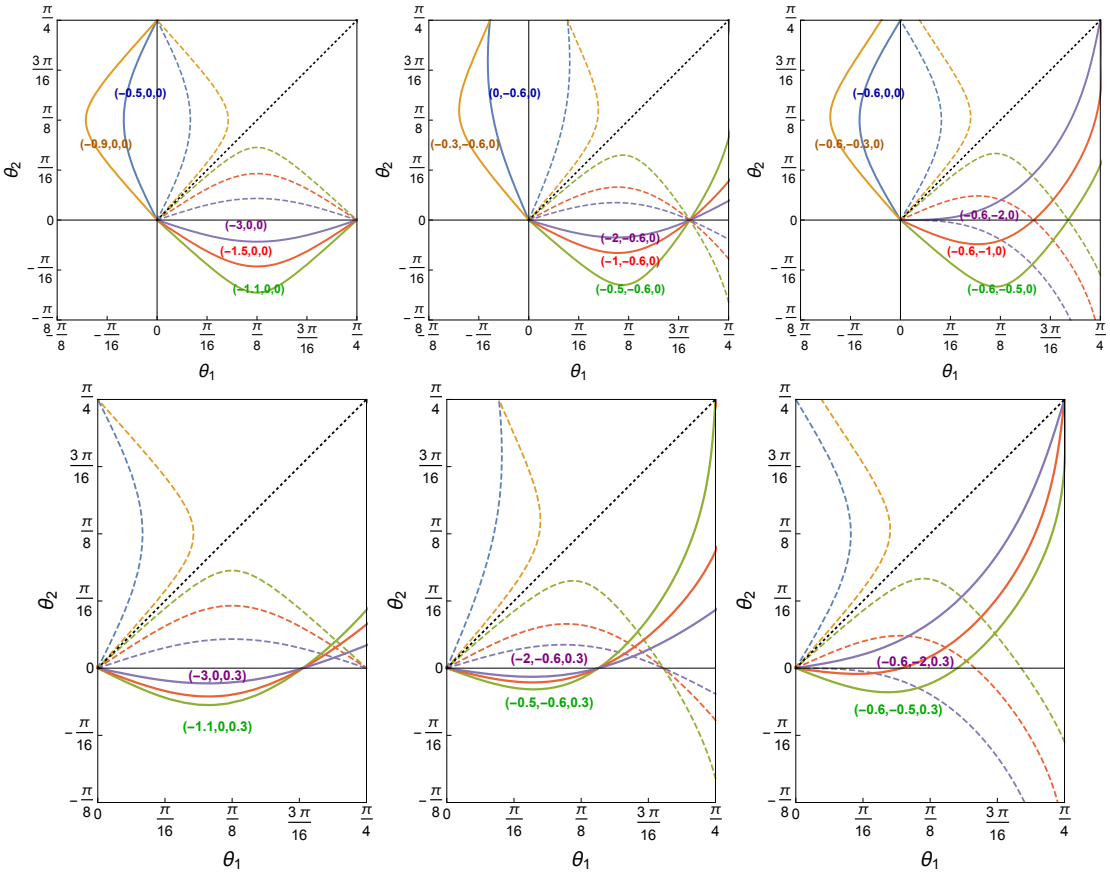

Figure 3: The contour lines show the relation between (θ_1, θ_2) imposed by the first (dashed lines) and second (solid lines) tadpole conditions. Each contour is labeled by the radiative parameters $(\Omega_1, \Omega_2, F_m)$. The left (middel) panel shows contours for different Ω_1 with $\Omega_2 = 0(-0.6)$. The right panel shows contours for different Ω_2 with $\Omega_1 = -0.6$. The upper and lower panels correspond to $F_m = 0$ and 0.3 respectively.

convex behaviour of the contours. From Fig. 2 (left and middel), the smaller Ω_1, the larger convex contour if $|\Omega_1 + \Omega_2| > 1$, while vice versa for $|\Omega_1 + \Omega_2| < 1$.

The second tadpole condition provides us another relation on (θ_1, θ_2), which is shown as another contour in the (θ_1, θ_2) plane. Together with the contour from first tadpole condition, the two contours uniquely determine value of (θ_1, θ_2) which is the intersection point between two contours. Similar to Fig. 2, let us plot the (θ_1, θ_2) contours imposed by the second tadpole condition. To clearly present the effects of each parameters, we first turn off tree-level breaking parameters (F_λ, F_m). In this case, the two conditions reduce to

$$\begin{aligned} &\sin 4\theta_1 + \Omega_1 \sin 4\theta_2 + \Omega_2 \sin 2(\theta_1 + \theta_2) = 0, \\ &\sin 4\theta_1 - \Omega_1 \sin 4\theta_2 + \Omega_2 \sin 2(\theta_1 - \theta_2) = 0. \end{aligned} \tag{4.12}$$

Fig. 3 shows the (θ_1, θ_2) contours imposed by two conditions for different (Ω_1, Ω_2). We note that the two conditions are symmetric under $\theta_1 \leftrightarrow -\theta_1$ if $|\Omega_1 + \Omega_2| > 1$, while they are symmetric under $\theta_2 \leftrightarrow -\theta_2$ if $|\Omega_1 + \Omega_2| < 1$. This symmetric behaviour can be seen from Fig. 3. Therefore we can determine the solution

for (θ_1, θ_2):

$$\begin{cases} \theta_2 = 0, \theta_1 \leq \pi/4, & \text{for } |\Omega_1 + \Omega_2| > 1 \\ \theta_1 = 0, \theta_2 \geq \pi/4, & \text{for } |\Omega_1 + \Omega_2| < 1. \end{cases} \tag{4.13}$$

This indicates only one Higgses H_i obtain VEV. From the left panel of the Fig. 3, if $\Omega_2 = 0$, we have either $\theta_1 = \pi/4$ (if $|\Omega_1 + \Omega_2| > 1$) or $\theta_2 = \pi/4$ (if $|\Omega_1 + \Omega_2| < 1$). According to the middle panel, when $\Omega_2 < 0$, we have either $\theta_1 < \pi/4$ (if $|\Omega_1 + \Omega_2| > 1$) or $\theta_2 > \pi/4$ (if $|\Omega_1 + \Omega_2| < 1$). On the right panel, it shows as Ω_2 decreases, the value of θ_1 decreases. Thus we could obtain appropriate asymmetric vacua θ_1 when we vary Ω_2. When we take $|\Omega_1 + \Omega_2| > 1$, θ_1 could be smaller than $\pi/4$ as we vary Ω_2. Thus even without tree-level breaking parameters, the vacuum misalignment could still happen. This is the scenario of radiative $\mathbb{Z}_2$ symmetry breaking [26].

Turning on tree-level breaking terms (F_λ, F_m) will change the contour curve between θ_1 and θ_2 imposed by the second tadpole condition. For simplicity, let us turn on one tree-level breaking term: F_λ or F_m. Fig. 3 (lower panel) shows the (θ_1, θ_2) contours imposed by two conditions for different $(\Omega_1, \Omega_2, F_m)$. For comparison, we use the same (Ω_1, Ω_2) in both the upper and lower panels of Fig. 3. We find that turning on F_m shifts the intersection point between the contour and the x-axis to lower θ_1, and also change the convex behavior of the contour. F_m plays a similar role as Ω_2. Fig. 3 (left) show that even Ω_2 is zero, turning on F_m will obtain the following solution:

$$\theta_2 < \theta_1 \leq \pi/4, \quad \text{for } |\Omega_1 + \Omega_2| > 1. \tag{4.14}$$

Thus vacuum misalignment could be realized via the bilinear term m_{12}^2. This is the scenario of tadpole induced $\mathbb{Z}_2$ symmetry breaking [24,25]. Furthermore, Fig. 3 (middle and right) show that turning on Ω_2 will also obtain the viable solution, with the feature: the larger Ω_2, the smaller θ_1. Finally, our discussion on the tree-level breaking term F_m could also apply to the case with only F_λ. The results are quite similar to the one in Fig. 3. In this case, the λ_{45} plays the role to obtain vacuum misalignment. This is the scenario of quartic induced $\mathbb{Z}_2$ symmetry breaking.

The set of parameters $(\Omega_1, \Omega_2, F_\lambda, F_m)$ only uniquely determine (θ_1, θ_2), but not the VEVs (v_1, v_2). To obtain the electroweak VEVs, additional condition (the VEV condition) needs to be imposed:

$$f_1^2 \sin^2\theta_1 + f_2^2 \sin^2\theta_2 = v^2, \tag{4.15}$$

where $v = 174$ GeV. Given t_β and $\theta_{1,2}$, we could determine f_1 and f_2. Fig. 4 (left) shows the VEV contours on the θ_1 and θ_2 plane for different f_1 and t_β. f_1 determines the intersection point between the curve and the x-axis, while t_β determines the bending behaviour of the curve. Fig. 4 (middle and right) shows that once t_β is fixed, f_1 could be determined and thus the VEV contour is fixed. There is one special case. In Fig. 4 (middle), when the tree-level breaking term is off, f_1 is the same for different t_β. Thus in radiative $\mathbb{Z}_2$ case, f_1 is determined by (Ω_1, Ω_2).

Let us estimate the range of the tree-level breaking parameters F_m, F_λ and global symmetry breaking scales $f_{1,2}$ if we would like to obtain $\theta_1 < \pi/4$. Fig. 5 (left) shows that value of F_m or F_λ which determines θ_1 for different t_β. Interestingly, even when F_m or F_λ is absent, we could still obtain $\theta_1 < \pi/4$, which corresponds to the radiative breaking scenario. Fig. 5 (right) shows that once we know θ_1 (and t_β), f_1 is determined. As t_β gets larger, the needed f_1 becomes larger. Note that this relation is quite general and

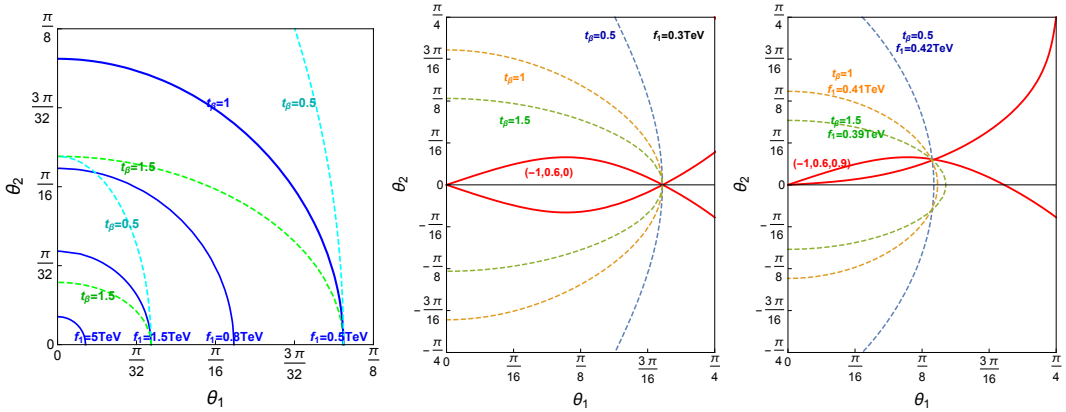

Figure 4: The solid contours on the (θ_1, θ_2) planes shows the VEV relations for fixed $t_\beta = 1.5$ and different $f_1 = 0.5, 0.75, 1, 2.5$ TeV. The dashed lines shows the VEV relations for different $t_\beta = 0.5, 1, 1.5, 2$ with fixed $f_1 = 0.5$ TeV (the left panel) and $f_1 = 1$ TeV (the right panel).

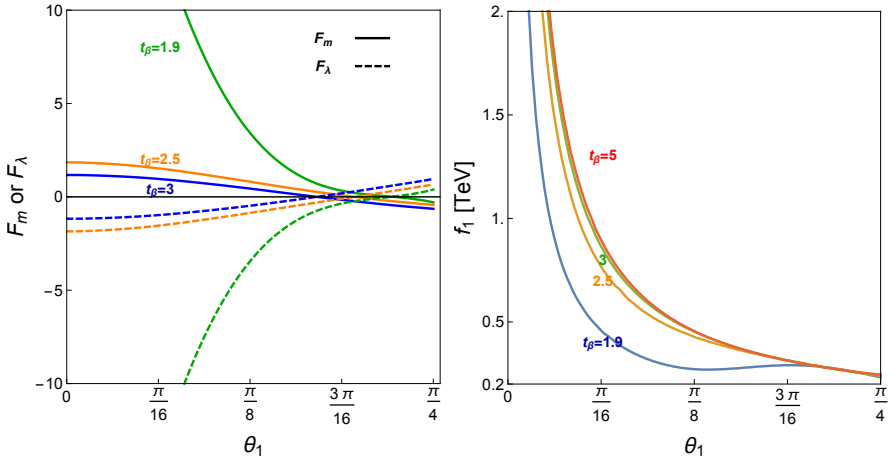

Figure 5: On the left panel, it shows the relations between θ_1, and F_m (solid lines) or F_λ (dashed lines). On the right panel, the contours shows the relations between θ_1 and f_1 imposed by the VEV condition for different t_β.

does not depend on scenarios. Thus in tadpole or quartic induced symmetry breaking, only two independent parameters are needed, which are typically taken to be $F_m(F_\lambda)$ and t_β. If there is no tree-level breaking term, only one parameter t_β could determine the VEVs.

Finally let us summarize what we have obtained so far from the tadpole conditions. The tadpole conditions determine (θ_1, θ_2), which depend on (Ω_1, Ω_2) and/or (F_m, F_λ). Given $\Omega_{1,2} \leq 0$, the vacuum misalignment requires $\theta_2 < \theta_1 < \pi/4$ with $|\Omega_1 + \Omega_2| > 1$. Three scenarios are discussed to obtain this misalignment. We classify these scenarios according to parameters (Ω_1, Ω_2) and (F_m, F_λ):

- Radiative $\mathbb{Z}_2$ breaking [26], when $\Omega_1 \neq 0, \Omega_2 \neq 0$. Since there is no tree-level breaking term, the

tree-level potential is $U(4) \times U(4)$ invariant:

$$V_{U(4)\times U(4)} = -\mu_1^2|H_1|^2 - \mu_2^2|H_2|^2 + \lambda_1(|H_1|^2)^2 + \lambda_2(|H_2|^2)^2 + \lambda_3|H_1|^2|H_2|^2. \quad (4.16)$$

The radiative corrections to the scalar potential are shown in Eq. 3.34. The Ω_1 determines whether the electroweak symmetry breaking could happen, while the Ω_2 determines whether vacuum misalignment could happen. Since $\Omega_1 < 0, \Omega_2 < 0$, the solution of the asymmetric vacua have $\theta_1 < \pi/4$ and $\theta_2 \equiv 0$. The two tadpole conditions reduce to one

$$\sin 4\theta_1 + \Omega_2 \sin 2(\theta_1) = 0. \quad (4.17)$$

Thus the θ_1 only depends on Ω_2: the larger Ω_2 the smaller θ_1. Although the gauge corrections are much smaller than the Yukawa corrections, Ω_2 could be large if $t_\beta \gg 1$. When Ω_2 approaches one, θ_1 approaches to zero.

- m_{12}^2-induced $\mathbb{Z}_2$ breaking [24, 25], when $\Omega_1 \neq 0, m_{12}^2 \neq 0$. The tree-level potential is

$$V_{\text{Tadpole}} = V_{U(4)\times U(4)} + m_{12}^2 \left[H_1^\dagger H_2 + h.c.\right]. \quad (4.18)$$

The dominant radiative corrections to the scalar potential are the same as the radiative $\mathbb{Z}_2$ breaking case. Similarly Ω_1 determines whether the electroweak symmetry breaking could happen. However, if t_β is not so large, only Ω_2 could not obtain small enough θ_1. In certain case Ω_2 could even disappear. The m_{12}^2 is needed to obtain appropriate θ_1. In this case it is the m_{12}^2 which determines whether vacuum misalignment could happen. As explained in Ref. and next section, the m_{12}^2 plays the role of the tadpole terms, which transit the value of θ_1 to θ_2, and thus the $\theta_1 < \pi/4$ is produced.

- λ_{45}-induced $\mathbb{Z}_2$ breaking, when $\Omega_1 \neq 0, \lambda_{45} \neq 0$. The tree-level potential is

$$V_{\text{Quartic}} = V_{U(4)\times U(4)} + \lambda_4|H_1^\dagger H_2|^2 + \lambda_5 \left[(H_1^\dagger H_2)^2 + h.c.\right]. \quad (4.19)$$

Similarly Ω_1 determines whether the electroweak symmetry breaking could happen. Although Ω_2 could exist, it is the $\lambda_{4,5}$ determines whether vacuum misalignment could happen. Negative $\lambda_{4,5}$ is favored to obtain appropriate θ_1.

It is also possible that both both m_{12}^2 and $\lambda_{4,5}$ terms exist in the potential. In this case, it is the m_{12}^2 and $\lambda_{4,5}$ which determine whether vacuum misalignment could happen. This is the mixture of the tadpole and quartic induced $\mathbb{Z}_2$ breaking scenarios.

5 Spontaneous $\mathbb{Z}_2$ Breakings in 2HDM Framework

In the above section, we discussed how the tadpole conditions determine the electroweak vacua (θ_1, θ_2). Three different mechanisms could lead to the vacuum misalignment $\theta_2 < \theta_1 < \pi/4$, and thus the spontaneous $\mathbb{Z}_2$ breaking. Let us understand the physics behind these $\mathbb{Z}_2$ breaking scenarios.

Since the electroweak symmetry breaking only involves in the PGBs in visible A sector, we will simplify the original scalar potential in Eq. 3.2 and Eq. 3.34 by setting

$$H_{1B} \simeq \begin{pmatrix} 0 \\ f_1 \cos\left(\frac{\mathbb{H}_1}{f_1}\right) \end{pmatrix}, \qquad H_{2B} \simeq \begin{pmatrix} 0 \\ f_2 \cos\left(\frac{\mathbb{H}_2}{f_2}\right) \end{pmatrix}. \quad (5.1)$$

Expanding the potential to the quartic order, we obtain the approximated visible sector potential in the 2HDM framework

$$\begin{aligned} V(H_{1A}, H_{2A}) &= -\mu_{1A}^2|H_{1A}|^2 - \mu_{2A}^2|H_{2A}|^2 + \lambda_{1A}|H_{1A}|^4 + \lambda_{2A}|H_{2A}|^4 + \lambda_{3A}|H_{1A}|^2|H_{2A}|^2 \\ &\quad + m_{A12}^2\left[H_{1A}^\dagger H_{2A} + h.c.\right] + \lambda_{4A}|H_{1A}^\dagger H_{2A}|^2 + \frac{\lambda_{5A}}{2}\left[(H_{1A}^\dagger H_{2A})^2 + h.c.\right] \\ &\quad + \left[(\lambda_{6A}|H_{1A}|^2 + \lambda_{7A}|H_{2A}|^2)H_{1A}^\dagger H_{2A} + h.c.\right]. \end{aligned} \tag{5.2}$$

All the coefficients in the potential are proportional to the tree-level and loop-induced breaking terms:

$$\begin{aligned} \mu_{1A}^2 &= 2\delta_1 f_1^2 + (\delta_{345} + \lambda_{45})f_2^2 + m_{12}^2 t_\beta, \\ \mu_{2A}^2 &= 2\delta_2 f_2^2 + (\delta_{345} + \lambda_{45})f_1^2 + m_{12}^2 t_\beta^{-1}, \\ \lambda_{1A} &= \frac{8\delta_1}{3} + \frac{\delta_{345} + \lambda_{45}}{3}t_\beta^2 + \frac{m_{12}^2}{12 f_1^2}t_\beta, \\ \lambda_{2A} &= \frac{8\delta_2}{3} + \frac{\delta_{345} + \lambda_{45}}{3}t_\beta^{-2} + \frac{m_{12}^2}{12 f_2^2}t_\beta^{-1}, \\ \lambda_{3A} &= \delta_{345} + \lambda_{45} + \frac{m_{12}^2}{2 f_1 f_2}, \\ m_{A12}^2 &= m_{12}^2 + \lambda_{45} f_1 f_2, \quad \lambda_{4A} = \lambda_4 + \delta_4, \quad \lambda_{5A} = \lambda_5 + \delta_5, \\ \lambda_{6A} &= \frac{2\lambda_{45}}{3}t_\beta + \frac{m_{12}^2}{6 f_1^2}, \quad \lambda_{7A} = \frac{2\lambda_{45}}{3}t_\beta^{-1} + \frac{m_{12}^2}{6 f_2^2}. \end{aligned} \tag{5.3}$$

Note that there is no dependence on the tree-level parameters λ_{1-3}.

5.1 Radiative $\mathbb{Z}_2$ Breaking

In this scenario, the tree-level breaking terms m_{12}^2 and $\lambda_{4,5}$ do not exist. From the above potential, the Higgs mass squared terms reduce to

$$\mu_{H_{1A}}^2 = f_1^2\left(2\delta_1 + \delta_{345}t_\beta^2\right), \quad \mu_{H_{2A}}^2 = f_2^2\left(2\delta_2 + \delta_{345}t_\beta^{-2}\right), \tag{5.4}$$

and the quartic terms reduce to

$$\lambda_{1A} = \frac{8\delta_1}{3} + \frac{\delta_{345}}{3}t_\beta^2, \quad \lambda_{2A} = \frac{8\delta_2}{3} + \frac{\delta_{345}}{3}t_\beta^{-2}. \tag{5.5}$$

Since H_{1A} has negative mass-squared $-\mu_{H_{1A}}^2 < 0$, H_{1A} gets VEV. While H_{2A} has positive mass-squared $-\mu_{H_{2A}}^2 > 0$, there is no VEV for H_{2A}. The potential reduces to the inert Higgs doublet potential [30]:

$$V_{\text{inert}} \supset \left[-|\mu_{1A}^2||H_{1A}|^2 + \lambda_{1A}|H_{1A}|^4\right] + \left[|\mu_{2A}^2||H_{2A}|^2 + \lambda_{2A}|H_{2A}|^4 + \delta_{345}|H_{1A}|^2|H_{2A}|^2\right], \tag{5.6}$$

where we neglect the $\delta_{4,5}$ contributions. The first two terms in the potential, determine the electroweak vacuum:

$$v^2 = \mu_{1A}^2/\lambda_{1A} \simeq \frac{3}{8}\left(2 + \delta_{345}t_\beta^2/\delta_1\right) f_1^2. \tag{5.7}$$

To obtain the electroweak VEV $v = 174$ GeV, the two terms should cancel with each other. We know although contributions δ_1 (from Yukawa corrections) and δ_{345} (from gauge corrections) have opposite sign, the adequate cancellation will not happen because typically $\delta_1 \gg \delta_{345}$. To have required cancellation, we

could utilize large t_β in the second term to enhance the second term in the mass-squared $\mu^2_{H_{2A}}$. At the same time, if λ_{1A} is not reduced compared to the mass-squared $\mu^2_{H_{2A}}$, the electroweak VEV is obtained.

Finally, we could read out the masses of the PGBs. The Higgs mass is

$$m_h^2 = 2\mu_{1A}^2 = \left(4\delta_1 + 2\delta_{345}t_\beta^2\right) f_1^2. \tag{5.8}$$

We could obtain the masses of the charged and neutral scalars in the inert doublet:

$$m^2_{H^\pm} \quad = \quad \mu^2_{2A} + \delta_{345}v^2, \quad m^2_{A^0} = \mu^2_{2A} + \delta_{345}v^2. \tag{5.9}$$

In typical 2HDM model, the masses of the charged and CP-odd neutral scalar are only proportional to $\delta_{4,5}$, which is very small. In this scenario, the inert scalar masses also have $\delta_{2,3}$ dependence, which induces a large mass for the inert scalars. Therefore, the radiative $\mathbb{Z}_2$ breaking scenario can be viewed as a natural UV completion of the inert Higgs doublet model.

5.2 Tadpole Induced $\mathbb{Z}_2$ Breaking

The radiative $\mathbb{Z}_2$ breaking scenario can only realize the electroweak symmetry breaking when δ_{345} is non-zero, and if the enhancement from $t_\beta \gg 1$ exists. Otherwise, the vacuum misalignment cannot be obtained by purely radiative $\mathbb{Z}_2$ breaking. The tadpole induced $\mathbb{Z}_2$ breaking scenario is suitable to the case with δ_{345} is zero, or $t_\beta \sim 1$. However, the price to pay is introducing additional m^2_{12} term.

Let us turn on m^2_{12} gradually to see how the VEVs $\theta_{1,2}$ vary. When m^2_{12} term is off, from the radiative breaking scenario, the VEVs have

$$\langle H_{1A}\rangle \simeq f_1, \quad \langle H_{2A}\rangle \simeq 0. \tag{5.10}$$

If $t_\beta \sim 1$, we obtain $\mu^2_{1A} \gg \mu^2_{2A}$ due to $\delta_1 \gg -\delta_{345}$. Thus m_{h_1} is much heavier than m_{h_2}. When gradually turning on m^2_{12} term, the h_2 starts to obtain small VEV. This can be seen from the potential assuming h_1 is too heavy and decoupled. After integrating out h_1, the potential generates an effective tadpole term. The h_2 potential is dominated by the tadpole and quadratic terms

$$V(H_{2A}) \quad \supset \quad \mu^2_{2A}h_2^2 + m^2_{12}f_1h_2 \tag{5.11}$$

Thus h_2 obtain VEV

$$\langle H_{2A}\rangle \sim m^2_{12}f_1/\mu^2_{2A}, \tag{5.12}$$

which gradually becomes large as m^2_{12} increases. At the same time, the VEV of h_1 decreases. This can be seen from the H_{1A} potential. Assuming the VEV $\langle h_2\rangle$ is small, the relevant H_{1A} potential is

$$V(H_{1A}) \quad \simeq \quad -\left(2\delta_1 f_1^2 + \delta_{345}f_2^2 + m^2_{12}t_\beta\right)|H_{1A}|^2 + \left(\frac{8\delta_1}{3} + \frac{\delta_{345}}{3}t_\beta^2 + \frac{m^2_{12}}{12f_1^2}t_\beta\right)|H_{1A}|^4. \tag{5.13}$$

Here the tadpole contribution is negligible due to $\langle h_1\rangle > \langle h_2\rangle$. From the potential, we see that as the m^2_{12} becomes larger, there are large cancellation in the quadratic term, which cause the VEV $\langle h_1\rangle$ becomes smaller. Therefore, the bilinear term m^2_{12} plays the role of an effective tadpole. As the effective tadpole term increases, the VEV θ_1 decreases from $\pi/4$, while the VEV θ_2 increases from 0. The vacuum misalignment $\theta_2 < \theta_1 < \pi/4$ could be realized when an appropriate m^2_{12} term is taken.

5.3 Quartic Induced $\mathbb{Z}_2$ Breaking

In this scenario, only quartic breaking terms $\lambda_{4,5}$ are in the tree level potential. Unlike the m_{12}^2 case, the quartic breaking scenario could be all the range of the t_β. The $\lambda_{4,5}$ terms appear in both quadratic term μ_{1A}^2 and the bilinear term. The quadratic term has

$$\mu_{1A}^2 = f_1^2 \left(2\delta_1 + (\delta_{345} + \lambda_{45})\, t_\beta^2\right). \tag{5.14}$$

We see that both δ_{345} and $\lambda_{4,5}$ contribute to cancel the opposite δ_1 corrections. At the same time, it generates the effective tadpole term, which transits the value of the VEV θ_1 to the one of the θ_2. Since it is similar to the above cases, it could generate the appropriate $\mathbb{Z}_2$ breaking.

6 Higgs Phenomenology

6.1 Higgs Mass Spectra

In this natural 2HDM framework, it contains two Higgs doublets H_{1A}, H_{2A} in A sector, and another two Higgs doublets H_{1B}, H_{2B} (with two neutral radial mode decoupled) in B sector. There are six exact GBs: three $(z^{\pm,0})$ from H_{iA} and three $(C^\pm, N^0)$ from H_{iB}. All of them are eaten by gauge bosons in A and B sectors. Depending on the breaking pattern, the other particles in the scalar multiplets could be PGBs or just scalar particles. We present the details of the mass spectra in two breaking pattern in Appendix A and B.

Here we summarize main features of the mass spectra based on results in Appendix A and B.

- Explicit Soft $\mathbb{Z}_2$ Breaking

  In the Higgs basis, the field H plays the role of twin Higgs, while another field H' is just additional scalar $U(4)$ multiplet. Thus among seven GBs, six are eaten by gauge bosons, and one PGB is the Higgs boson. For the additional scalars in H', the masses are

$$\begin{aligned} m_{H^\pm}^2 &= m_A^2 = \frac{m_{12}^2 + m_{12A}^2}{s_\beta c_\beta} - \frac{1}{2}(\lambda_4 + \lambda_5) f^2, \\ m_{H'^\pm}^2 &= m_{A'}^2 = \frac{m_{12}^2}{s_\beta c_\beta} - \lambda_5 f^2. \end{aligned} \tag{6.1}$$

  which only depends on $U(4)$ breaking parameters m_{12}^2, m_{12A}^2 and $\lambda_{4,5}$ in the potential. If the tree-level terms $\lambda_{4,5}$ do not exist, then all the new scalars have degenerate masses. In SUSY extension of the twin Higgs model, the mass spectra are much simplified.

- Radiative $\mathbb{Z}_2$ Breaking

  The global symmetry breaking is $[U(4) \times U(4)] \to [U(3) \times U(3)]$. All the scalar components in visible sector are PGBs. Furthermore, since only H_{1A} obtains VEV, H_{2A} is an inert Higgs doublet. In the twin sector, since both H_{1B} and H_{2B} have VEVs, the PGBs in twin sector have mixing. The PGBs mass eigenstates have

$$\begin{aligned} m_{H^\pm}^2 &= -2\delta_2 f_2^2 - \delta_{345} f_1^2 \cos 2\theta_1 - \delta_{45} f_1^2 \sin^2\theta_1, \qquad m_{H'^\pm}^2 = -\delta_{45}(f_1^2 \cos^2\theta_1 + f_2^2), \\ m_{A^0}^2 &= -2\delta_2 f_2^2 - \delta_{345} f_1^2 \cos 2\theta_1 - 2\delta_5 f_1^2 \sin^2\theta_1, \qquad m_{A'^0}^2 = -2\delta_5(f_1^2 \cos^2\theta_1 + f_2^2). \end{aligned} \tag{6.2}$$

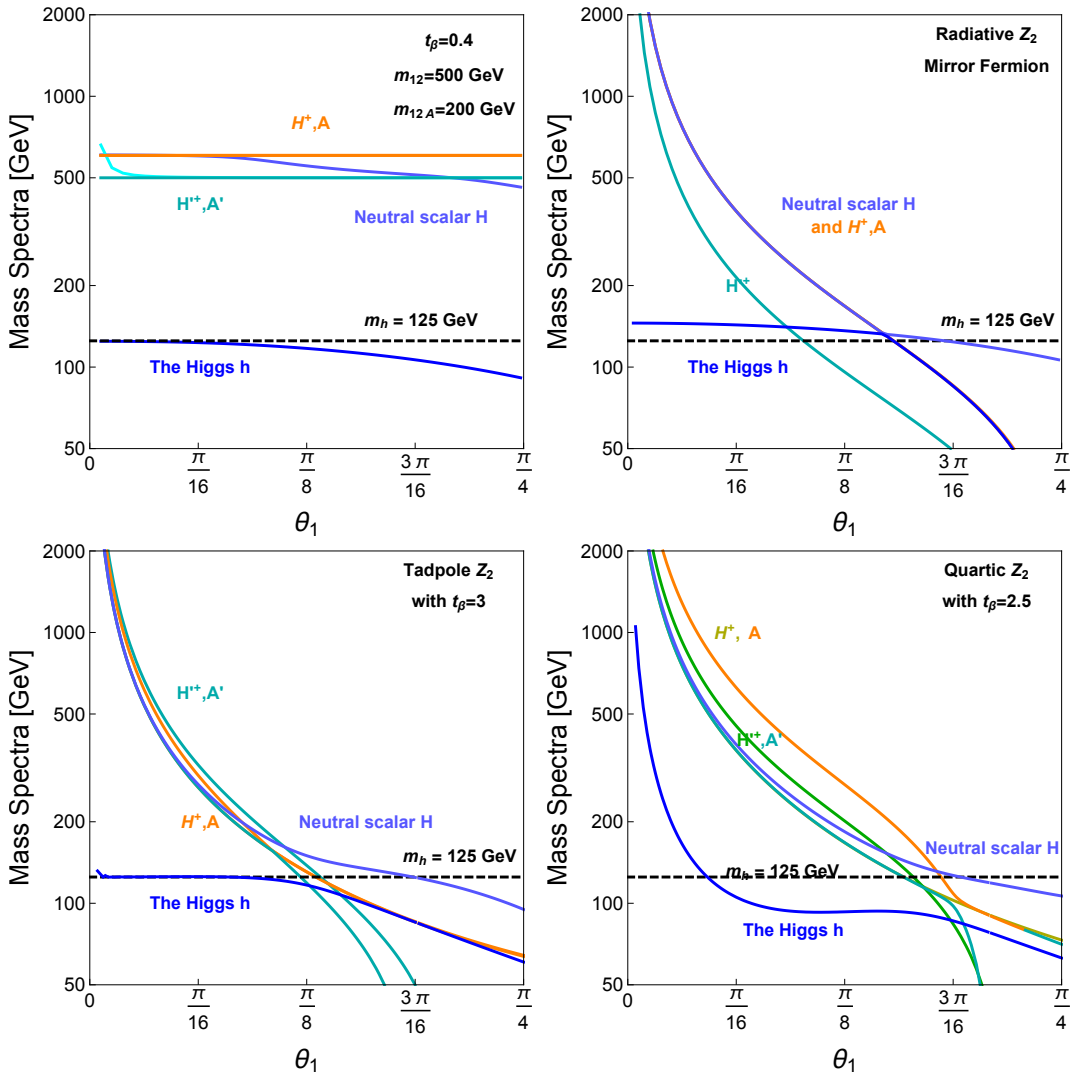

Figure 6: The masses spectra as the function of θ_1 in four $\mathbb{Z}_2$ breaking scenarios. The particles in the mass spectra are charge and neutral CP odd Higgses $(H^\pm, A^0)$ in visible sector, charged and neutral CP odd Higgses $(H'^\pm, A'^0)$ in twin sector, and two CP even Higgses (h, H) in visible sector.

- Tadpole-Induced $\mathbb{Z}_2$ Breaking

  Similar to the radiative breaking scenario, all the scalars except the radial modes in two two Higgs doublets are PGBs. The difference is that there are mixing between two Higgs doublet in A sector, with mixing angle β_A, defined in Appendix B. All the masses of the charged Higgses and CP odd Higgses depend on m_{12}^2 and are nearly degenerate when $\theta_{1,2}$ are much smaller than $\pi/4$. The mass spectra read

$$\begin{aligned} m_{H^\pm}^2 &= m_{A_1^0}^2 = \frac{m_{12}^2}{f_1 \sin\theta_1 f_2 \sin\theta_2} \left(f_1^2 \sin^2\theta_1 + f_2^2 \sin^2\theta_2\right), \\ m_{H'^\pm}^2 &= m_{A_2^0}^2 = \frac{m_{12}^2}{f_1 \cos\theta_1 f_2 \cos\theta_2} \left(f_1^2 \cos^2\theta_1 + f_2^2 \cos^2\theta_2\right). \end{aligned} \tag{6.3}$$

- Quartic-Induced $\mathbb{Z}_2$ Breaking

  Similar to the tadpole induced breaking scenario, all the masses of the charged Higgses and CP odd Higgses depend on $\lambda_{4,5}$. The difference is that there are mass splitting between charged and neutral CP odd Higgses unless $\lambda_4 = \lambda_5$. The charged scalar masses are

$$\begin{aligned} m^2_{H^\pm} &= -\lambda_{45}(1+\cot\theta_1\cot\theta_2)\left(f_1^2\sin^2\theta_1 + f_2^2\sin^2\theta_2\right), \\ m^2_{H'^\pm} &= -\lambda_{45}(1+\tan\theta_1\tan\theta_2)\left(f_1^2\cos^2\theta_1 + f_2^2\cos^2\theta_2\right). \end{aligned} \tag{6.4}$$

  and the CP-odd scalar masses are presented in Appendix B.

In all scenarios, the SM Higgs boson origins from the mixing between h_1 and h_2 in visible sector. The exception is that in radiative breaking scenario, there is no mixing between h_1 and h_2. The Higgs mass is proportional to all the breaking parameters δ_{1-5} and/or $m^2_{12}(\lambda_{4,5})$. We present the mass matrices of the Higgs boson in Appendix A and B. Fig. 6 shows the mass spectra in the above four scenarios. The independent parameters in four scenarios are taken to be $(\theta_1, t_\beta, m_{12} = 500, m_{12A} = 200)$ (explicit Z_2 breaking), θ_1 (radiative breaking), $\theta_1, t_\beta = 3$ (tadpole breaking), and $\theta_1, t_\beta = 2.8$ (quartic breaking). Fig. 6 shows that typically charge and neutral CP odd Higgses $(H^\pm, A^0)$ in visible sector have degenerate masses, and similarly for charged and neutral CP odd Higgses $(H'^\pm, A'^0)$ in twin sector. If we want to obtain 125 GeV Higgs boson mass, this will give us additional constraint on the model parameters. Fig. 6 shows that once we fix other parameters in the model, θ_1 is determined by the requirement of the 125 GeV mass of the Higgs boson.

6.2 Collider Constraints

Let us first consider the visible sector. The visible sector contains the same particle contents as the 2HDM. The phenomenology in visible sector should be very similar to the one in 2HDM, except that there could be additional decay channels to the twin particles. For simplicity, we take the Type-I Yukawa structure in this work, although other Yukawa structure, such as Type-II, X, Y, are possible. Let us setup the notation similar to 2HDM. According to the Appendix A and B, the 2HDM mixing angles and electroweak VEV are different in two breaking patterns, defined as

$$U(4)/U(3) \equiv \begin{cases} \beta = \frac{f_2}{f_1}, & \text{mixing angle between charged/CP-odd scalars,} \\ v = f\sin\theta, & \text{electroweak vacuum,} \\ \alpha, & \text{mixing angle between CP even scalars,} \end{cases} \tag{6.5}$$

$$U(4)^2/U(3)^2 \equiv \begin{cases} \beta_A = \frac{f_2\sin\theta_2}{f_1\sin\theta_1}, & \text{mixing angle between charged/CP-odd scalars,} \\ v = \sqrt{f_1\sin\theta_1 + f_2\sin\theta_2}, & \text{electroweak vacuum,} \\ \alpha, & \text{mixing angle between CP even scalars.} \end{cases} \tag{6.6}$$

Note that the definition of the mixing angle α is opposite from the typical notation, such as Ref. [28]. The normalized Higgs couplings to the SM gauge bosons and fermions are

$$\kappa_{hVV} \equiv \frac{g_{hVV}}{g^{\rm SM}_{hVV}} = \begin{cases} \cos\theta c_{\alpha-\beta}, & \text{Explicit } \mathbb{Z}_2 \text{ Breaking,} \\ \cos\theta_1, & \text{Radiative } \mathbb{Z}_2 \text{ Breaking,} \\ \cos\theta_1 c_\alpha c_{\beta_A} + \cos\theta_2 s_\alpha s_{\beta_A}, & \text{Tadpole and Quartic } \mathbb{Z}_2 \text{ Breaking,} \end{cases} \tag{6.7}$$

$$\kappa_{hff} \equiv \frac{y_{hff}}{y_{hff}^{\rm SM}} = \begin{cases} \cos\theta \frac{c_\alpha}{c_\beta}, & \text{Explicit } \mathbb{Z}_2 \text{ Breaking}, \\ \cos\theta_1, & \text{Radiative } \mathbb{Z}_2 \text{ Breaking}, \\ \cos\theta_1 \frac{c_\alpha}{c_{\beta_A}}, & \text{Tadpole and Quartic } \mathbb{Z}_2 \text{ Breaking}. \end{cases} \tag{6.8}$$

Here the SM couplings are taken to be $g_{hVV}^{\rm SM} = \frac{2m_V^2}{v}$ and $g_{hff}^{\rm SM} = \frac{m_f}{v}$. These Higgs couplings are constrained by the Higgs coupling measurements at the LHC. The charged and CP-odd neutral scalars in visible sector have the same constraints as the one in 2HDM. On the other hand, the CP-even neutral scalars need to take the decays to twin particles into account.

The twin sector contains another two Higgs doublet $H_{1B,2B}$, the mirror gauge bosons, and mirror fermions. The mirror gauge bosons are mirror photon, and mirror W_B, Z_B, which absorb three GBs in two Higgs doublets. For simplicity, two radial modes in $H_{1B,2B}$ are assumed to be decoupled. The physical scalars in twin sector are charged and neutral CP odd scalars $H'^{\pm}, A'^0$. The mirror fermions could induce very rich twin hadron phenomenology [31] because they are charged under the mirror QCD. Since the twin fermions are mirror copy of the SM particles, the mirror fermion phenomenology should be similar to the original twin Higgs. For simplicity, we take the fermion setup in the fraternal twin Higgs model [31], and leave more general discussion for future. The fermionic ingredients of the fraternal twin Higgs setup are summarized as follows:

- To avoid the twin $SU(3)$ and twin $SU(2)$ anomalies, the whole third generation twin fermions are introduced: twin top, bottom, tau, and twin tau neutrino, but not first two generations;
- The fermion Yukawa interactions are taken to be the fermion assignment I in our discussion;
- The twin $SU(3)$ has confinement, which indicates the existence of the twin glue-balls, and twin bottomonium and hadrons below confinement scalar $\Lambda_3' \sim \mathcal{O}(10)\Lambda_{\rm QCD}$.

To be specific, we take the twin bottom Yukawa coupling the same as the bottom Yukawa coupling, which indicates $m_{b^B} \simeq m_b \frac{f}{v}$. Thus the Higgs boson could decay into b_B: $h \to b_B \bar{b}_B$. Because twin fermions are SM charge neutral, some of them could be dark matter candidate. This has been discussed in Refs. [31–33].

The Higgs boson and the heavier CP even neutral scalar provide connection between visible and twin sector. The Higgs boson also couples to the twin particles because it is a PGB. Here we denote the VEV in twin sector $v' \equiv f\cos\theta$ ($v' \equiv \sqrt{f_1^2\cos\theta_1^2 + f_2^2\cos\theta_2^2}$), and mixing angle β (β_B) in explicit (spontaneous) breaking pattern. The normalized Higgs couplings to the twin gauge bosons and fermions are

$$\kappa'_{hVV} \equiv \frac{g_{hV_BV_B}}{g_{hV_BV_B}^{\rm SM}} = \begin{cases} \sin\theta c_{\alpha-\beta}, & \text{Explicit } \mathbb{Z}_2 \text{ Breaking}, \\ \sin\theta_1, & \text{Radiative } \mathbb{Z}_2 \text{ Breaking}, \\ \sin\theta_1 c_\alpha c_{\beta_B} + \sin\theta_2 s_\alpha s_{\beta_B}, & \text{Tadpole and Quartic } \mathbb{Z}_2 \text{ Breaking}, \end{cases} \tag{6.9}$$

$$\kappa'_{hff} \equiv \frac{y_{hf_Bf_B}}{y_{hf_Bf_B}^{\rm SM}} = \begin{cases} \sin\theta \frac{c_\alpha}{c_\beta}, & \text{Explicit } \mathbb{Z}_2 \text{ Breaking}, \\ \sin\theta_1, & \text{Radiative } \mathbb{Z}_2 \text{ Breaking}, \\ \sin\theta_1 \frac{c_\alpha}{c_{\beta_B}}, & \text{Tadpole and Quartic } \mathbb{Z}_2 \text{ Breaking}. \end{cases} \tag{6.10}$$

Here the SM-like couplings are taken to be $g_{hV_BV_B}^{\rm SM} = \frac{2m_{V_B}^2}{v'}$ and $g_{hf_Bf_B}^{\rm SM} = \frac{m_{f_B}}{v'}$. The Higgs invisible decay channels are $h \to f_B\bar{f}_B, V_BV_B, A_BA_B$. Since in general the normalized couplings of the Higgs boson to the

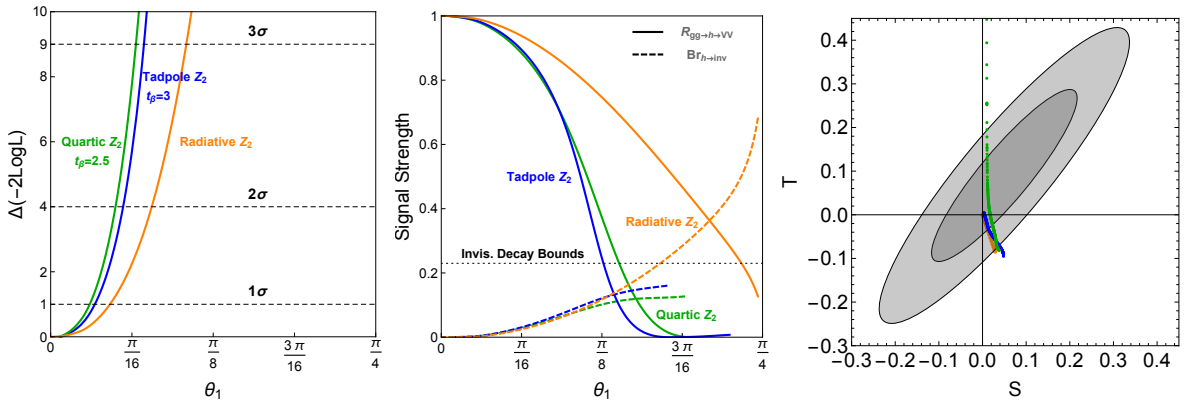

Figure 7: On the left, it shows the log-likelihood profile $\Delta(-2\log\mathcal{L})$ as the function of θ_1 in three scenarios. Here $1\sigma, 2\sigma, 3\sigma$ errors are also shown. On the middle, it shows the signal strength in gluon fusion production and subsequent VV decays, and Higgs invisible branching ratio as function of θ_1 in three scenarios. The bound on the invisible decay branching ratio is $\mathrm{Br}_{\mathrm{inv}} < 0.23$. On the right, the $S-T$ oblique parameter contours at the $1\sigma, 2\sigma$ levels are shown. The dotted points are the parameter points in three scenarios: radiative (orange color), tadpole (blue), and quartic (green) $\mathbb{Z}_2$ breaking scenarios.

twin gauge bosons and fermions are different, we can not do a simple scaling on the signal strength. We calculate the Higgs invisible decay widths based on the above couplings.

We take the latest LHC results on the Higgs coupling measurements [34,35] and Higgs invisible decays [36], and perform a global fit on the model parameters. In the tadpole and quartic $\mathbb{Z}_2$ breaking scenarios, if we fix the parameter t_β, only one free parameter exists. Thus in all the spontaneous $\mathbb{Z}_2$ breaking scenarios, we will vary θ_1 and fix other parameters. Furthermore, we will not consider the explicit breaking scenario, since it should be less constrained than the other three scenarios. In the following, we utilize the Lilith package [37] to perform a global fitting on the Higgs signal strength. In the case where the Higgs coupling measurements are well within the Gaussian statistical regime, the likelihood function is defined

$$-2\log\mathcal{L}(\mu) = \chi^2(\mu) = \sum_{i=1}^{n} \frac{[\mu_i - \hat{\mu}_i(\theta_1)]^2}{\Delta\mu_i}. \tag{6.11}$$

Based on Higgs signal strengths at the 8 TeV LHC with 20.7 fb^{-1} data [34], a statistical analysis is performed by the Lilith package. Fig. 7 (left panel) shows the log-likelihood profile $\Delta(-2\log\mathcal{L})$ as the function of θ_1, in three scenarios. Here in tadpole and quartic scenarios we fix the parameter $t_\beta = 3$ and $t_\beta = 2.5$. Up to the 2σ level, the exclusion limits in three scenarios are that θ_1 should typically be less than 0.2. This put very strong constraints on the model parameter. Looking back to Fig. 6, we note that both this Higgs coupling constraints and the requirement on 125 GeV Higgs mass should be satisfied. The tadpole and quartic breaking scenarios are viable, but the radiative breaking scenario has the tension between the Higgs coupling constraints and the 125 GeV Higgs boson mass requirement. If the $U(4)$ fermion assignment is taken in the radiative breaking scenario, there will not have such tension, and there are θ_1 which could satisfy both conditions. This viable fermion assignment has been discussed in Ref. [26]. Although the invisible decay width has been taken into account indirectly in the above global fitting, we would like to

consider constraints from the direct searches on the Higgs invisible decays. The updated upper limits on the invisible decay branching ratio is $\mathrm{Br}_{\mathrm{inv}} < 0.23$ [36]. Fig. 7 (middle panel) shows the invisible decay branching ratio as the function of θ_1. As a comparison, we also plot the signal strength in the gluon fusion process $gg \to h_1 \to VV$. From the Figure, we see that the direct searches on the invisible decays put much weaker constraints than the Higgs coupling measurements. The high luminosity LHC will improve sensitivity of signal strengths to around 5% assuming current uncertainty with 3 ab^{-1} luminosity [38]. Thus we should be able to explore more parameter regions at the high luminosity LHC.

According to the updated results on oblique parameters via Gfitter package [39], the S, T parameters have $S = 0.05 \pm 0.09, T = 0.11 \pm 0.13$, with correlation coefficients of $+0.90$ between S and T. In this model, the S and T parameters contains two contributions: corrections from possible radial modes, and corrections from 2HDM scalars. The corrections from radial modes takes the form

$$\Delta S \simeq \frac{1}{6\pi} \sin^2\theta \log\frac{m_\rho}{m_h}, \quad \Delta T \simeq -\frac{3}{8\pi c_W^2} \sin^2\theta \log\frac{m_\rho}{m_h}, \tag{6.12}$$

with radial modes ρ, while the 2HDM corrections [40] are roughly

$$\Delta S \simeq \frac{m_H^2 + m_A^2 - 2m_{H^\pm}^2}{24\pi m_A^2}, \quad \Delta T \simeq \frac{(m_{H^\pm}^2 - m_A^2)(m_{H^\pm}^2 - m_H^2}{48\pi s_W^2 m_W^2 m_A^2}. \tag{6.13}$$

In our numerical study, the complete form of the S, T parameters [28, 40] are used. From the above, we see that if the radial modes decouple, or if the heavy scalars are degenerate, the first or the second correction will be negligible. Fig. 7 (right panel) plots the predicted S, T values in three scenarios, which we vary the parameter θ_1 while fixing $t_\beta = 3$ in tadpole scenario, and $t_\beta = 2.5$ in tadpole scenario. According to the $S - T$ oblique parameter contours at the $1\sigma, 2\sigma$ levels, we note that most of the S, T values are within the 2σ level contour. Thus the precision electroweak test can not provide tighter constraints on the model parameters than the one from the Higgs coupling measurements.

Let us briefly discuss the distinct signatures of this model. First, like the original twin Higgs model, the twin hadron phenomenology [31] provides us very distinct signatures from other models. Furthermore, the additional charged and neutral scalars provide us a way to distinguish this model from the original twin Higgs. This has been explored in the 2HDM contents for general case [28] and inert case [41]. Finally, to distinguish it from the typical 2HDM, the signatures from the twin $H'^\pm$ and A'^0 need to be explored. Furthermore, if the radial modes are not so heavy (thus not decoupled), exploring the radial mode decay channels could provide us different signatures from the typical 2HDM model. The detailed collider phenomenology would require studies of their own. We leave the detailed study in future.

7 Conclusions

In this work, we investigated a class of two twin Higgs models, in which the Higgs sector is extended to incorporate two twin Higgses and the global symmetry breaking pattern could be either $U(4) \to U(3)$ or $[U(4) \times U(4)] \to [U(3) \times U(3)]$. The SM Higgs boson is identified as one of the pseudo Goldstone Bosons after symmetry breaking. The discrete $\mathbb{Z}_2$ symmetry protects the Higgs mass term against the quadratically divergent radiative corrections. However, the $\mathbb{Z}_2$ symmetry needs to be broken to generate electroweak scale, which should be separated from the new physics scale. Typically the soft or hard explicit $\mathbb{Z}_2$ breaking terms

are introduced to do so. We found that in the two twin Higgs setup, it is possible to realize spontaneous $\mathbb{Z}_2$ breaking, without the need of explicit $\mathbb{Z}_2$ breaking terms.

We performed a systematical study on the general $\mathbb{Z}_2$ breaking conditions in a natural two Higgs doublet framework, and discussed various possible scenarios which could realize the vacuum misalignment. In the radiative $\mathbb{Z}_2$ breaking scenario, given the appropriate fermion assignments, the $\mathbb{Z}_2$ symmetry could be spontaneously broken purely due to the radiative corrections to the Higgs potential. In this scenario, only one Higgs obtains the electroweak vacuum, and the other is just an inert Higgs. The tadpole-induced $\mathbb{Z}_2$ breaking scenario can also be classified in this two Higgs doublet framework. In this scenario, the bilinear term in the scalar potential triggers the spontaneous $\mathbb{Z}_2$ breaking. We also proposed a novel scenario: the quartic-induced $\mathbb{Z}_2$ breaking scenario. In this scenario, the $\lambda_{4,5}$ terms instead of the bilinear term in the scalar potential trigger the spontaneous $\mathbb{Z}_2$ breaking.

In the two twin Higgs models, we discussed phenomenology of the Higgs sector in the two Higgs doublet framework. Although particle contents in the scalar sector are the same, the Higgs mass spectra are quite distinct for each $\mathbb{Z}_2$ breaking scenarios. The radiative $\mathbb{Z}_2$ breaking scenario includes an inert Higgs doublet with degenerated masses. Both the tadpole-induced and quartic-induced $\mathbb{Z}_2$ breaking scenarios contain additional scalars in two Higgs doublet model with not so degenerated masses. We calculated various Higgs couplings and utilized the the Higgs coupling measurements at the current LHC to constrain the model parameters. The additional scalars from the Higgs sector should be able to be probed at the Run-2 LHC and future colliders.

Acknowledgements

The author would like to thank Can Kilic and Nathaniel Craig for valuable discussions. This work was supported by DOE Grant DE-SC0011095.

A Details in the $U(4)/U(3)$ Breaking Pattern

In this breaking pattern, the scalar potential takes the form

$$\begin{aligned}
V_{U(4)} &= -\mu_1^2|H_1|^2 - \mu_2^2|H_2|^2 + \lambda_1(|H_1|^2)^2 + \lambda_2(|H_2|^2)^2 + \lambda_3|H_1|^2|H_2|^2 \\
&\quad + m_{12}^2\left[H_1^\dagger H_2 + h.c.\right] + \lambda_4|H_1^\dagger H_2|^2 + \lambda_5\left[(H_1^\dagger H_2)^2 + h.c.\right], \\
V_{\text{rad.cor.}} &= +\delta_1\left(|H_{1A}|^4 + |H_{1B}|^4\right) + \delta_2\left(|H_{2A}|^4 + |H_{2B}|^4\right) + \delta_3\left(|H_{1A}|^2|H_{2A}|^2 + |H_{1B}|^2|H_{2B}|^2\right) \\
&\quad + \delta_4\left(|H_{1A}^\dagger H_{2A}|^2 + |H_{1B}^\dagger H_{2B}|^2\right) + \frac{\delta_5}{2}\left[(H_{1A}^\dagger H_{2A})^2 + (H_{1B}^\dagger H_{2B})^2 + h.c.\right], \\
V_{\text{soft}} &= -m_{1A}^2|H_{1A}|^2 - m_{2A}^2|H_{2A}|^2 - m_{12A}^2\left[H_{1A}^\dagger H_{2A} + h.c.\right].
\end{aligned} \tag{A.1}$$

As a special case, the supersymmetric extension of the twin Higgs model is one specific realization in this breaking pattern. We identify the specific terms in the scalar potential [20] in SUSY twin Higgs model as

$$\begin{aligned}
&\mu_1^2 = -(m_{H_u}^2 + \mu^2), \quad \mu_2^2 = -(m_{H_d}^2 + \mu^2), \quad m_{12}^2 = -b, \\
&\lambda_{1,2,3,5} = 0, \quad \lambda_4 = \lambda^2, \quad \delta_1 = \delta_2 = \frac{\delta_3}{2} = \frac{g^2 + g'^2}{8}, \quad \delta_{4,5} = 0.
\end{aligned} \tag{A.2}$$

Thus all our discussion about $U(4)/U(3)$ breaking pattern can be applied to the SUSY twin Higgs model.

The tadpole conditions are

$$\begin{aligned}
\mu_1^2 &= \frac{f_2}{f_1}m_{12}^2 + (\delta_1+2\lambda_1)f_1^2 + (\lambda_{345}+\delta_{345}/2)\,f_2^2 + \left(f_1^2\delta_1 + f_2^2\delta_{345}/2\right)\cos 2\theta,\\
\mu_2^2 &= \frac{f_1}{f_2}m_{12}^2 + (\delta_2+2\lambda_2)f_2^2 + (\lambda_{345}+\delta_{345}/2)\,f_1^2 + \left(f_2^2\delta_2 + f_1^2\delta_{345}/2\right)\cos 2\theta,\\
m_{1A}^2 &= -\frac{f_2}{f_1}m_{12A}^2 + \left(f_1^2\delta_1 + f_2^2\delta_{345}\right)\cos 2\theta,\\
m_{2A}^2 &= -\frac{f_1}{f_2}m_{12A}^2 + \left(f_2^2\delta_2 + f_1^2\delta_{345}\right)\cos 2\theta.
\end{aligned} \tag{A.3}$$

Similar to the 2HDM, rotating to the Higgs basis

$$H = H_1\cos\beta + H_2\sin\beta, \qquad H' = -H_1\sin\beta + H_2\cos\beta. \tag{A.4}$$

In the Higgs basis, the masses of the charged gauge bosons are

$$\begin{aligned}
m_{G^\pm}^2 &= m_{C^\pm}^2 = 0, \quad \text{(Goldstone Bosons)},\\
m_{H^\pm}^2 &= \left(\frac{m_{12A}^2+m_{12}^2}{f_1f_2} - \delta_{45}\sin^2\theta - \lambda_{45}\right)(f_1^2+f_2^2),\\
m_{H'^\pm}^2 &= \left(\frac{m_{12}^2}{f_1f_2} - \delta_{45}\cos^2\theta - \lambda_{45}\right)(f_1^2+f_2^2).
\end{aligned} \tag{A.5}$$

The mass matrices of the neutral CP-odd gauge bosons are

$$\begin{aligned}
m_{G^0}^2 &= m_{N^0}^2 = 0, \quad \text{(Goldstone Bosons)},\\
m_{A^0A^0}^2 &= \left(\frac{m_{12A}^2+m_{12}^2}{f_1f_2} - 2\delta_5\sin^2\theta - (\lambda_4-\lambda_5)\cos^2\theta - 2\lambda_5\right)(f_1^2+f_2^2),\\
m_{A'^0A'^0}^2 &= \left(\frac{m_{12}^2}{f_1f_2} - 2\delta_5\cos^2\theta - (\lambda_4-\lambda_5)\sin^2\theta - 2\lambda_5\right)(f_1^2+f_2^2),\\
m_{A^0A'^0}^2 &= \frac{\lambda_4-\lambda_5}{2}\sin 2\theta(f_1^2+f_2^2),
\end{aligned} \tag{A.6}$$

Performing a further rotation on the fields (A^0, A'^0), we obtain the mass eigenvalues

$$m_{A,A'}^2 = m_{A^0A^0}^2 + m_{A'^0A'^0}^2 \pm \sqrt{(m_{A^0A^0}^2 - m_{A'^0A'^0}^2)^2 - 4m_{A^0A'^0}^4}. \tag{A.7}$$

Assuming radial mode H'^0 is heavy, the mass matrices of the CP-even gauge bosons are

$$\begin{aligned}
m_{h^0h^0}^2 &= 4\delta_1 f_1^2\sin^2\theta + \frac{f_2(m_{12}^2+m_{12A}^2)}{f_1} - \lambda_{45}f_2^2\cos^2\theta,\\
m_{H^0H^0}^2 &= 4\delta_2 f_2^2\sin^2\theta + \frac{f_1(m_{12}^2+m_{12A}^2)}{f_2} - \lambda_{45}f_1^2\cos^2\theta,\\
m_{h^0H^0}^2 &= -m_{12}^2 - m_{12A}^2 + \lambda_{45}f_1f_2 + (2\delta_{345}+\lambda_{45})f_1f_2\sin^2\theta.
\end{aligned} \tag{A.8}$$

Similar to 2HDM, we could further rotate the field with a rotation angle $\alpha-\beta$:

$$\begin{pmatrix} h \\ H \end{pmatrix} = \begin{pmatrix} c_{\alpha-\beta} & s_{\alpha-\beta} \\ -s_{\alpha-\beta} & c_{\alpha-\beta} \end{pmatrix}\begin{pmatrix} h^0 \\ H^0 \end{pmatrix}, \tag{A.9}$$

we obtain the mass eigenstates

$$m_{h,H}^2 = m_{h^0h^0}^2 + m_{H^0H^0}^2 \mp \sqrt{(m_{h^0h^0}^2 - m_{H^0H^0}^2)^2 - 4m_{h^0H^0}^4}. \tag{A.10}$$

Here we identify h as the SM Higgs boson.

B Details in the $[U(4)\times U(4)]\,/\,[U(3)\times U(3)]$ Breaking Pattern

The general scalar potential reads

$$\begin{aligned}
V_{U(4)\times U(4)} &= -\mu_1^2|H_1|^2-\mu_2^2|H_2|^2+\lambda_1(|H_1|^2)^2+\lambda_2(|H_2|^2)^2+\lambda_3|H_1|^2|H_2|^2,\\
V_{\rm breaking} &= m_{12}^2\left[H_1^\dagger H_2+h.c.\right]+\lambda_4|H_1^\dagger H_2|^2+\frac{\lambda_5}{2}\left[(H_1^\dagger H_2)^2+h.c.\right]\\
V_{\rm rad.cor.} &= \delta_1\left(|H_{1A}|^4+|H_{1B}|^4\right)+\delta_2\left(|H_{2A}|^4+|H_{2B}|^4\right)+\delta_3\left(|H_{1A}|^2|H_{2A}|^2+|H_{1B}|^2|H_{2B}|^2\right)\\
&+ \delta_4\left(|H_{1A}^\dagger H_{2A}|^2+|H_{1B}^\dagger H_{2B}|^2\right)+\frac{\delta_5}{2}\left[(H_{1A}^\dagger H_{2A})^2+(H_{1B}^\dagger H_{2B})^2+h.c.\right]. \qquad \text{(B.1)}
\end{aligned}$$

Here due to existence of the small tree-level breaking terms, the $U(4)\times U(4)$ symmetry is approximate.

The tadpole conditions are

$$\mu_1^2 = (\delta_1+2\lambda_1)f_1^2+\frac{1}{2}(\delta_{345}+2\lambda_3+\lambda_{45})f_2^2+\frac{\sin 2\theta_2}{2\sin 2\theta_1}\lambda_{45}f_2^2-\frac{f_2\sin(\theta_1+\theta_2)}{f_1\sin 2\theta_1}m_{12}^2, \qquad \text{(B.2)}$$

$$\mu_2^2 = (\delta_2+2\lambda_2)f_2^2+\frac{1}{2}(\delta_{345}+2\lambda_3+\lambda_{45})f_1^2+\frac{\sin 2\theta_1}{2\sin 2\theta_2}\lambda_{45}f_1^2-\frac{f_1\sin(\theta_1+\theta_2)}{f_2\sin 2\theta_2}m_{12}^2, \qquad \text{(B.3)}$$

and

$$f_1^4\delta_1\sin 4\theta_1+f_2^4\delta_2\sin 4\theta_2 = -f_1^2f_2^2\delta_{345}\sin 2(\theta_1+\theta_2), \qquad \text{(B.4)}$$

$$f_1^4\delta_1\sin 4\theta_1-f_2^4\delta_2\sin 4\theta_2 = 4f_1f_2m_{12}^2\sin(\theta_1-\theta_2)-f_1^2f_2^2(\delta_{345}+2\lambda_{45})\sin 2(\theta_1-\theta_2). \qquad \text{(B.5)}$$

Similar to the 2HDM, let us define the mixing angles of the VEVs in the A and B sectors

$$\tan\beta_A=\frac{f_2\sin\theta_2}{f_1\sin\theta_1},\qquad \tan\beta_B=\frac{f_2\cos\theta_2}{f_1\cos\theta_1}. \qquad \text{(B.6)}$$

Then we will perform a rotation from the H_1, H_2 basis

$$\begin{aligned}
&\begin{pmatrix} h^\pm \\ H^\pm \end{pmatrix}=\begin{pmatrix} \cos\beta_A & \sin\beta_A \\ -\sin\beta_A & \cos\beta_A \end{pmatrix}\begin{pmatrix} h_1^\pm \\ h_2^\pm \end{pmatrix}, \qquad \begin{pmatrix} C^\pm \\ H'^\pm \end{pmatrix}=\begin{pmatrix} \cos\beta_B & \sin\beta_B \\ -\sin\beta_B & \cos\beta_B \end{pmatrix}\begin{pmatrix} C_1^\pm \\ C_2^\pm \end{pmatrix},\\
&\begin{pmatrix} z^0 \\ A_1^0 \end{pmatrix}=\begin{pmatrix} \cos\beta_A & \sin\beta_A \\ -\sin\beta_A & \cos\beta_A \end{pmatrix}\begin{pmatrix} {\rm Im}h_1^0 \\ {\rm Im}h_2^0 \end{pmatrix}, \qquad \begin{pmatrix} N^0 \\ A_2^0 \end{pmatrix}=\begin{pmatrix} \cos\beta_B & \sin\beta_B \\ -\sin\beta_B & \cos\beta_B \end{pmatrix}\begin{pmatrix} N_1^0 \\ N_2^0 \end{pmatrix}. \qquad \text{(B.7)}
\end{aligned}$$

The charged mass spectra have

$$\begin{aligned}
m_{C^\pm}^2 &= m_{h^\pm}^2=0, \quad \text{(exact Goldstone bosons)},\\
m_{H^\pm}^2 &= -\left(f_1^2\sin^2\theta_1+f_2^2\sin^2\theta_2\right)\left[\delta_{45}+\lambda_{45}(1+\cot\theta_1\cot\theta_2)-\frac{m_{12}^2}{f_1\sin\theta_1 f_2\sin\theta_2}\right],\\
m_{H'^\pm}^2 &= -\left(f_1^2\cos^2\theta_1+f_2^2\cos^2\theta_2\right)\left[\delta_{45}+\lambda_{45}(1+\tan\theta_1\tan\theta_2)-\frac{m_{12}^2}{f_1\cos\theta_1 f_2\cos\theta_2}\right]. \qquad \text{(B.8)}
\end{aligned}$$

Similarly, the CP-odd neutral masses have

$$\begin{aligned}
m_{N^0}^2 &= m_{z^0}^2=0, \quad \text{(exact Goldstone bosons)},\\
m_{A_1^0}^2 &= -\left(f_1^2\sin^2\theta_1+f_2^2\sin^2\theta_2\right)\left[2\delta_5+2\lambda_5+\lambda_{45}\cot\theta_1\cot\theta_2-\frac{m_{12}^2}{f_1\sin\theta_1 f_2\sin\theta_2}\right],\\
m_{A_2^0}^2 &= -\left(f_1^2\cos^2\theta_1+f_2^2\cos^2\theta_2\right)\left[2\delta_5+2\lambda_5+\lambda_{45}\tan\theta_1\tan\theta_2-\frac{m_{12}^2}{f_1\cos\theta_1 f_2\cos\theta_2}\right],
\end{aligned}$$

$$m^2_{A^0_1 A^0_2} = (\lambda_4 - \lambda_5)\sqrt{\left(f_1^2 \sin^2\theta_1 + f_2^2 \sin^2\theta_2\right)\left(f_1^2\cos^2\theta_1 + f_2^2\cos^2\theta_2\right)}. \quad \text{(B.9)}$$

Note that there is still mixing between (A^0_1, A^0_2), a further rotation from (A^0_1, A^0_2) to the mass eigenstates (A^0, A'^0) are needed with the mass eigenstates

$$m^2_{A^0, A'^0} = m^2_{A^0_1} + m^2_{A^0_2} \pm \sqrt{(m^2_{A^0_1} - m^2_{A^0_2})^2 - 4m^4_{A^0_1 A^0_2}}. \quad \text{(B.10)}$$

Finally, we obtain the masses for the SM-like Higgs boson and heavier Higgs boson. Assuming the radial modes are heavy, we obtain the the 2×2 mass matrices in the $\mathrm{Re}\, h^0_1, \mathrm{Re}\, h^0_2$ basis

$$\mathcal{M}^2_{\rm Higgs} = \begin{pmatrix} m^2_{h_1 h_1} & m^2_{h_1 h_2} \\ m^2_{h_1 h_2} & m^2_{h_2 h_2} \end{pmatrix}. \quad \text{(B.11)}$$

The mass matrices read

$$\begin{aligned}
m^2_{h_1 h_1} &= \frac{\delta_1 f_1^2}{2}(1 - 3\cos 4\theta_1) - \frac{\delta_{345} f_2^2}{2}\cos 2\theta_1 \cos 2\theta_2 - \frac{\lambda_{45} f_2^2}{2}\frac{\sin(4\theta_1 - 2\theta_2) + 3\sin 2\theta_2}{\sin 2\theta_1} + \frac{m^2_{12} f_2}{f_1}\frac{\sin(\theta_1 + \theta_2)}{\sin 2\theta_1}, \\
m^2_{h_2 h_2} &= \frac{\delta_2 f_2^2}{2}(1 - 3\cos 4\theta_2) - \frac{\delta_{345} f_1^2}{2}\cos 2\theta_1 \cos 2\theta_2 - \frac{\lambda_{45} f_1^2}{2}\frac{\sin(4\theta_2 - 2\theta_1) + 3\sin 2\theta_1}{\sin 2\theta_2} + \frac{m^2_{12} f_1}{f_2}\frac{\sin(\theta_1 + \theta_2)}{\sin 2\theta_2}, \\
m^2_{h_1 h_2} &= \frac{\delta_{345} f_1 f_2}{2}\cos 2(\theta_1 + \theta_2) + \frac{(\delta_{345} + \lambda_{45}) f_1 f_2}{2}\cos 2(\theta_1 - \theta_2) - m^2_{12}\cos(\theta_1 - \theta_2). \quad \text{(B.12)}
\end{aligned}$$

Similar to 2HDM, let us rotate the (h_1, h_2) to the mass eigenstates (h, H) with rotation angle α:

$$\begin{pmatrix} h \\ H \end{pmatrix} = \begin{pmatrix} \cos\alpha & \sin\alpha \\ -\sin\alpha & \cos\alpha \end{pmatrix}\begin{pmatrix} h_1 \\ h_2 \end{pmatrix}. \quad \text{(B.13)}$$

Here the rotation angle is defined as

$$\tan 2\alpha = \frac{2m^2_{h_1 h_2}}{m^2_{h_1 h_1} - m^2_{h_2 h_2}}, \quad \text{(B.14)}$$

and the mass eigenvalues are

$$m^2_{h,H} = m^2_{h_1} + m^2_{h_2} \pm \sqrt{(m^2_{h_1} - m^2_{h_2})^2 - 4m^4_{h_1 h_2}}. \quad \text{(B.15)}$$

Here we identify h as the SM Higgs boson.

References

[1] G. Aad *et al.* [ATLAS Collaboration], Phys. Lett. B **716**, 1 (2012) doi:10.1016/j.physletb.2012.08.020 [arXiv:1207.7214 [hep-ex]].

[2] S. Chatrchyan *et al.* [CMS Collaboration], Phys. Lett. B **716**, 30 (2012) doi:10.1016/j.physletb.2012.08.021 [arXiv:1207.7235 [hep-ex]].

[3] R. Barbieri and A. Strumia, hep-ph/0007265.

[4] S. P. Martin, Adv. Ser. Direct. High Energy Phys. **21**, 1 (2010) [Adv. Ser. Direct. High Energy Phys. **18**, 1 (1998)] doi:10.1142/9789812839657, 10.1142/9789814307505 [hep-ph/9709356].

[5] D. B. Kaplan and H. Georgi, Phys. Lett. B **136**, 183 (1984). doi:10.1016/0370-2693(84)91177-8

[6] K. Agashe, R. Contino and A. Pomarol, Nucl. Phys. B **719**, 165 (2005) doi:10.1016/j.nuclphysb.2005.04.035 [hep-ph/0412089].

[7] N. Arkani-Hamed, A. G. Cohen, E. Katz and A. E. Nelson, JHEP **0207**, 034 (2002) doi:10.1088/1126-6708/2002/07/034 [hep-ph/0206021].

[8] Z. Chacko, H. S. Goh and R. Harnik, Phys. Rev. Lett. **96**, 231802 (2006) doi:10.1103/PhysRevLett.96.231802 [hep-ph/0506256]; JHEP **0601**, 108 (2006) doi:10.1088/1126-6708/2006/01/108 [hep-ph/0512088].

[9] G. Burdman, Z. Chacko, H. S. Goh and R. Harnik, JHEP **0702**, 009 (2007) doi:10.1088/1126-6708/2007/02/009 [hep-ph/0609152].

[10] H. Cai, H. C. Cheng and J. Terning, JHEP **0905**, 045 (2009) doi:10.1088/1126-6708/2009/05/045 [arXiv:0812.0843 [hep-ph]].

[11] Z. Chacko, H. S. Goh and R. Harnik, JHEP **0601**, 108 (2006) doi:10.1088/1126-6708/2006/01/108 [hep-ph/0512088].

[12] N. Craig, S. Knapen and P. Longhi, Phys. Rev. Lett. **114**, no. 6, 061803 (2015) doi:10.1103/PhysRevLett.114.061803 [arXiv:1410.6808 [hep-ph]]; JHEP **1503**, 106 (2015) doi:10.1007/JHEP03(2015)106 [arXiv:1411.7393 [hep-ph]].

[13] G. Burdman, Z. Chacko, R. Harnik, L. de Lima and C. B. Verhaaren, Phys. Rev. D **91**, no. 5, 055007 (2015) doi:10.1103/PhysRevD.91.055007 [arXiv:1411.3310 [hep-ph]].

[14] N. Craig, A. Katz, M. Strassler and R. Sundrum, JHEP **1507**, 105 (2015) doi:10.1007/JHEP07(2015)105 [arXiv:1501.05310 [hep-ph]].

[15] R. Barbieri, T. Gregoire and L. J. Hall, hep-ph/0509242.

[16] B. Bellazzini, C. Cski and J. Serra, Eur. Phys. J. C **74**, no. 5, 2766 (2014) doi:10.1140/epjc/s10052-014-2766-x [arXiv:1401.2457 [hep-ph]].

[17] Z. Chacko, Y. Nomura, M. Papucci and G. Perez, JHEP **0601**, 126 (2006) doi:10.1088/1126-6708/2006/01/126 [hep-ph/0510273].

[18] H. S. Goh and S. Su, Phys. Rev. D **75**, 075010 (2007) doi:10.1103/PhysRevD.75.075010 [hep-ph/0611015].

[19] S. Chang, L. J. Hall and N. Weiner, Phys. Rev. D **75**, 035009 (2007) doi:10.1103/PhysRevD.75.035009 [hep-ph/0604076].

[20] N. Craig and K. Howe, JHEP **1403**, 140 (2014) doi:10.1007/JHEP03(2014)140 [arXiv:1312.1341 [hep-ph]].

[21] P. Batra and Z. Chacko, Phys. Rev. D **79**, 095012 (2009) doi:10.1103/PhysRevD.79.095012 [arXiv:0811.0394 [hep-ph]].

[22] R. Barbieri, D. Greco, R. Rattazzi and A. Wulzer, JHEP **1508**, 161 (2015) doi:10.1007/JHEP08(2015)161 [arXiv:1501.07803 [hep-ph]].

[23] M. Low, A. Tesi and L. T. Wang, Phys. Rev. D **91**, 095012 (2015) doi:10.1103/PhysRevD.91.095012 [arXiv:1501.07890 [hep-ph]].

[24] H. Beauchesne, K. Earl and T. Grgoire, JHEP **1601**, 130 (2016) doi:10.1007/JHEP01(2016)130 [arXiv:1510.06069 [hep-ph]].

[25] R. Harnik, K. Howe and J. Kearney, arXiv:1603.03772 [hep-ph].

[26] J. H. Yu, arXiv:1608.01314 [hep-ph].

[27] H. C. Cheng, S. Jung, E. Salvioni and Y. Tsai, JHEP **1603**, 074 (2016) doi:10.1007/JHEP03(2016)074 [arXiv:1512.02647 [hep-ph]].

[28] G. C. Branco, P. M. Ferreira, L. Lavoura, M. N. Rebelo, M. Sher and J. P. Silva, Phys. Rept. **516**, 1 (2012) doi:10.1016/j.physrep.2012.02.002 [arXiv:1106.0034 [hep-ph]].

[29] N. Craig, S. Knapen, P. Longhi and M. Strassler, JHEP **1607**, 002 (2016) doi:10.1007/JHEP07(2016)002 [arXiv:1601.07181 [hep-ph]].

[30] R. Barbieri, L. J. Hall and V. S. Rychkov, Phys. Rev. D **74**, 015007 (2006) doi:10.1103/PhysRevD.74.015007 [hep-ph/0603188].

[31] N. Craig and A. Katz, JCAP **1510**, no. 10, 054 (2015) doi:10.1088/1475-7516/2015/10/054 [arXiv:1505.07113 [hep-ph]].

[32] I. Garca Garca, R. Lasenby and J. March-Russell, Phys. Rev. D **92**, no. 5, 055034 (2015) doi:10.1103/PhysRevD.92.055034 [arXiv:1505.07109 [hep-ph]];Phys. Rev. Lett. **115**, no. 12, 121801 (2015) doi:10.1103/PhysRevLett.115.121801 [arXiv:1505.07410 [hep-ph]].

[33] M. Farina, JCAP **1511**, no. 11, 017 (2015) doi:10.1088/1475-7516/2015/11/017 [arXiv:1506.03520 [hep-ph]].

[34] G. Aad *et al.* [ATLAS Collaboration], Eur. Phys. J. C **76**, no. 1, 6 (2016) doi:10.1140/epjc/s10052-015-3769-y [arXiv:1507.04548 [hep-ex]].

[35] V. Khachatryan *et al.* [CMS Collaboration], Eur. Phys. J. C **75**, no. 5, 212 (2015) doi:10.1140/epjc/s10052-015-3351-7 [arXiv:1412.8662 [hep-ex]].

[36] G. Aad *et al.* [ATLAS Collaboration], JHEP **1511**, 206 (2015) doi:10.1007/JHEP11(2015)206 [arXiv:1509.00672 [hep-ex]].

[37] J. Bernon and B. Dumont, Eur. Phys. J. C **75**, no. 9, 440 (2015) doi:10.1140/epjc/s10052-015-3645-9 [arXiv:1502.04138 [hep-ph]].

[38] ATLAS Collaboration, ATL-PHYS-PUB-2013-014, CERN, Geneva, Oct, 2013.

[39] M. Baak *et al.* [Gfitter Group Collaboration], Eur. Phys. J. C **74**, 3046 (2014) doi:10.1140/epjc/s10052-014-3046-5 [arXiv:1407.3792 [hep-ph]].

[40] H. E. Haber and D. O'Neil, Phys. Rev. D **83**, 055017 (2011) doi:10.1103/PhysRevD.83.055017 [arXiv:1011.6188 [hep-ph]].

[41] N. Blinov, J. Kozaczuk, D. E. Morrissey and A. de la Puente, Phys. Rev. D **93**, no. 3, 035020 (2016) doi:10.1103/PhysRevD.93.035020 [arXiv:1510.08069 [hep-ph]].